eNeuro

Research Article: New Research

Sensory and Motor Systems

A Transcription Factor Etv1/Er81 Is Involved in the Differentiation of Sweet, Umami, and Sodium Taste Cells

Makoto Ohmoto, Masafumi Jyotaki, Karen K. Yee, and Ichiro Matsumoto

https://doi.org/10.1523/ENEURO.0236-22.2023

Monell Chemical Senses Center, Philadelphia, PA 19104

Abstract

Taste cells are maintained by continuous turnover throughout a lifetime, yet the mechanisms of taste cell differentiation, and how taste sensations remain constant despite this continuous turnover, remain poorly understood. Here, we report that a transcription factor Etv1 (also known as Er81) is involved in the differentiation of taste cells responsible for the preference for sweet, umami, and salty tastes. Molecular analyses revealed that *Etv1* is expressed by a subset of taste cells that depend on Skn-1a (also known as Pou2f3) for their generation and express T1R genes (responsible for sweet and umami tastes) or *Scnn1a* (responsible for amiloride-sensitive salty taste). *Etv1*$^{CreERT2/CreERT2}$ mice express Etv1 isoform(s) but not Etv1 in putative proprioceptive neurons as comparable to wild-type mice, yet lack expression of Etv1 or an isoform in taste cells. These *Etv1*$^{CreERT2/CreERT2}$ mice have the same population of Skn-1a-dependent cells in taste buds as wild-type mice but have altered gene expression in taste cells, with regional differences. They have markedly decreased electrophysiological responses of chorda tympani nerves to sweet and umami tastes and to amiloride-sensitive salty taste evoked by sodium cation, but they have unchanged responses to bitter or sour tastes. Our data thus show that Etv1 is involved in the differentiation of the taste cells responsible for sweet, umami, and salty taste preferences.

Key words: Etv1; salty; sweet; taste cell; umami

Significance Statement

The sense of taste plays important roles in food choice by detecting beneficial (i.e., nutritional) and potentially harmful substances. Senescent taste cells are replaced throughout an animal's life by new ones generated from stem cells in the oral epithelia. However, the molecular mechanisms underlying taste cell turnover are poorly understood. By examining gene expression in taste cells and neural responses to taste substances, we found that the transcription factor Etv1 regulates the differentiation of sweet, umami, and salty taste cells. These findings advance our understanding of the molecular mechanisms underlying taste cell homeostasis and provide new insights into taste cell lineage.

Introduction

The sense of taste plays a key role in food choice. Individual taste cells of vertebrate animals primarily respond to only one taste (Yarmolinsky et al., 2009; Matsumoto et al., 2013); thus, the diversity of tastes that an animal can perceive depends on the diversity of taste cells present. Mice can distinguish five basic tastes: sweet by cells co-expressing *Tas1r2* and *Tas1r3* or expressing *Tas1r3* alone, umami (i.e., savory) by cells that co-express *Tas1r1* and *Tas1r3*, bitter by *Tas2r*-expressing cells, sour by *Pkd2l1*-expressing cells, and salty by cells that express the amiloride-sensitive Na^+ channel ENaC

Received June 18, 2022; accepted April 6, 2023; First published April 12, 2023.
The authors declare no competing financial interests.

Author contributions: M.O. and I.M. designed research; M.O., M.J., K.K.Y., and I.M. performed research; M.O., M.J., and I.M. analyzed data; M.O. and I.M. wrote the paper.

(Nelson et al., 2001, 2002; Zhao et al., 2003; Mueller et al., 2005; Huang et al., 2006; Chandrashekar et al., 2010; Ohmoto et al., 2020a). Taste cells can be distinguished from one another by their molecular features, especially by the expression of specific taste receptors, although no unique molecular markers specific for amiloride-sensitive salty taste cells (hereafter referred as sodium-taste cells) have been found, because ENaC subunit genes are also expressed in other taste cells (Chandrashekar et al., 2010; Nomura et al., 2020).

Taste cells emerge from local epithelial stem cells that express *Krt5* and *Sox2*, and their diverse populations are maintained by continuous turnover throughout an animal's life (Beidler and Smallman, 1965; Farbman, 1980; Stone et al., 1995; Ohmoto et al., 2017, 2020b). The transcription factor Skn-1a (also known as Pou2f3) specifies the fate of a cell as a sweet, umami, bitter, or sodium taste cell lineage, rather than a sour lineage, probably at the late precursor stage (Matsumoto et al., 2011; Ohmoto et al., 2020a). However, the molecular and cellular mechanisms underlying how these cells then differentiate into different functional taste cells of the specified lineage remain elusive.

Etv1 (also known as Er81), a transcription factor of the ETS family, is one such candidate for this process. In the nervous system it is involved in the terminal differentiation of peripheral and central neurons, such as proprioceptive sensory neurons and cerebellar granule neurons (Arber et al., 2000; Patel et al., 2003; Abe et al., 2011; Fleming et al., 2016; Okazawa et al., 2016). Etv1 is also required for the survival of proprioceptive sensory neurons with various degrees of dependence among proprioceptive sensory neurons (Patel et al., 2003) but not for the survival of granule cells in cerebellum or their formation of synaptic connections (Abe et al., 2011).

Etv1 is significantly enriched in taste buds of the rhesus macaque, and its expression is as high as that of taste-bud-specific transcription factor genes in tongue epithelium (Hevezi et al., 2009). Recent RNA sequencing data of taste cells support the presence of *Etv1* in *Tas1r3*$^{+}$ sweet taste cells but not in bitter or sour taste cells (Lee et al., 2017; Sukumaran et al., 2017). However, it remains unclear whether sodium-taste cells or nonsensory taste bud cells express *Etv1* or whether all *Tas1r3*$^{+}$ taste cells express it.

In the present study, we demonstrate that Etv1 is involved in differentiation of Skn-1a-dependent taste cells (i.e., often referred to as Type II cells): *Etv1* is expressed in sweet, umami, and sodium taste cells. Genetic ablation of Etv1 markedly decreases the expression of T1R genes in taste buds and culminates in the loss or reduction of responses to sweet and umami tastes in gustatory nerve recordings in mice. Etv1 ablation also represses *Scnn1a* expression and amiloride-sensitive salt taste responses in gustatory nerves. Sweet, umami, and sodium taste cells are still present in *Etv1*-deficient taste buds, but their populations are smaller than in heterozygous control mice.

Materials and Methods

Animals

C57BL/6J (stock #000664), homozygous B6.Cg-*Gt(ROSA)26Sor*$^{tm14(CAG-tdTomato)Hze}$/J (*Rosa26*$^{LSL-tdTomato}$, stock #007914; Madisen et al., 2010), and heterozygous B6(Cg)-*Etv1*$^{tm1.1(cre/ERT2)Zjh}$/J (*Etv1*$^{CreERT2/+}$, stock #013048; Taniguchi et al., 2011) strains were purchased from the Jackson Laboratory (for details of allele structure, see Fig. 2C). *Etv1*$^{CreERT2/CreERT2}$ (denoted as *Etv1*$^{C/C}$) mice were generated by crossing heterozygous (i.e., *Etv1*$^{CreERT2/+}$, denoted as *Etv1*$^{C/+}$) males and females and maintained by crossing homozygous mice. *Skn-1a*$^{-/-}$ mice with a C57BL/6J congenic background (i.e., B6.129-*Pou2f3*^{tm1Abek}) were generated in a previous study (Ohmoto et al., 2020a) and maintained by crossing homozygous mice. *Etv1*$^{C/C}$ mice and *Rosa26*$^{LSL-tdTomato}$ (denoted as *R26*$^{LSL-tdTom/LSL-tdTom}$) mice were mated to obtain *Etv1*$^{C/+}$; *R26*$^{LSL-tdTom/+}$ mice, which were then mated with *Etv1*$^{C/C}$ mice to obtain *Etv1*$^{C/C}$; *R26*$^{LSL-tdTom/+}$ mice. *Etv1*$^{C/+}$; *R26*$^{LSL-tdTom/+}$ and *Etv1*$^{C/C}$; *R26*$^{LSL-tdTom/+}$ mice that received tamoxifen, which caused tdTomato to label *Etv1*$^{+}$ cells, are denoted as *Etv1*$^{C/+}$; *R26*$^{Tom/+}$ and *Etv1*$^{C/C}$; *R26*$^{Tom/+}$, respectively. For embryo staging, the middle of the light period on the day of the vaginal plug was designated as embryonic day 0.5. All the mice used in this study had a C57BL/6J genetic background. Both sexes were used in all animal experiments, which were conducted according to a protocol approved by the Institutional Animal Care and Use Committee of the Monell Chemical Senses Center.

Tamoxifen administration

Tamoxifen (10 mg/ml in corn oil; Sigma-Aldrich) was injected intraperitoneally in mice (100 mg/kg body weight) once a day for five consecutive days. The mice were euthanized 1 d after the last tamoxifen injection.

Tissue preparation

Oral epithelia were dissected from mice deeply anesthetized by urethane, and sensory ganglia were dissected from mice that had been transcardially perfused with ice-cold PBS under anesthesia. Freshly dissected tissues were quickly embedded and frozen in optimal cutting temperature (O.C.T.) compound (Sakura Finetech). For tissues fixed with 4% paraformaldehyde (PFA), mice were deeply

This work was supported, in part, by National Institutes of Health (NIH) Grants R01DC015491 and R01DC017503 (to I.M.). This work was performed, in part, at the Monell Core Facilities, which were supported in part by the NIH-National Institute on Deafness and Other Communication Disorders Core Grant P30DC011735 and the Shared Instrument Award S10 OD030354.

M. Ohmoto's present address: Department of Nutrition, Faculty of Health and Welfare, Takasaki University of Health and Welfare, Takasaki, Gunma 370-0033, Japan.

Acknowledgments: We thank Dr. Hirohito Miura (Kagoshima University) for *Tas2r126* plasmid.

Correspondence should be addressed to Ichiro Matsumoto at imatsumoto@monell.org.

https://doi.org/10.1523/ENEURO.0236-22.2023

anesthetized with urethane and transcardially perfused with PBS followed by 4% PFA in PBS. For the developing neurons in the dorsal root ganglia (DRG), embryos were harvested from pregnant mice and fixed with 4% PFA, and lumber spinal columns including spinal cord and DRG were dissected. Dissected oral epithelia and embryonic spinal columns were postfixed, cryoprotected, and frozen as previously described (Ohmoto et al., 2008). Cryosections (8-μm thickness) were prepared using a CM1900 cryostat (Leica Microsystems), mounted on tissue adhesive-coated glass slides (Fisher Scientific), and preserved at −80°C until use.

In situ hybridization

In situ hybridization using fresh-frozen or PFA-fixed sections was conducted as previously described (Ohmoto et al., 2008, 2020a). Digoxigenin-labeled and fluorescein-labeled antisense RNAs were synthesized and used as probes after fragmentation to ~150 bases under alkaline conditions. The probe regions are shown in Table 1. For the *Tas2r* gene probes, riboprobes of *Tas2r104*, *Tas2r105*, *Tas2r118*, and *Tas2r126* were mixed. Fresh-frozen sections were fixed with 4% PFA and treated with diethylpyrocarbonate. The PFA-fixed sections were treated with proteinase K (3 μg/ml, Thermo Fisher Scientific), postfixed with 4% PFA, and then acetylated with acetic anhydride. The sections were prehybridized with salmon testis DNA, hybridized with the riboprobes for 40 h, and washed in 0.2× saline sodium citrate at 58°C, except when using the riboprobes for *Calhm1* and *Scnn1a*, for which sections were hybridized and washed at 65°C. After washing, chromogenic and/or fluorescent signals were developed as follows.

For single-label *in situ* hybridization, the chromogenic signals of the hybridized probes were detected using alkaline phosphatase-conjugated anti-digoxigenin antibodies (Roche Diagnostics, 11093274910, RRID:AB_514497) followed by 4-nitro blue tetrazolium chloride/5-bromo-4-chloro-3-indolyl phosphate as a substrate. The signals were developed overnight except for *Calhm1* probes, which were developed for 2 d. Short-term signal development for *Tas1r3* was also investigated at 4 h. Stained images were obtained using a Nikon Eclipse 80i microscope equipped with a DXM1200C digital camera (Nikon Instruments).

For double-fluorescence *in situ* hybridization in oral epithelia, the fluorescent signals of the riboprobes were developed using alkaline phosphatase-conjugated anti-digoxigenin antibodies followed by the HNPP Fluorescent Detection Set (Roche Diagnostics) and biotin-conjugated anti-fluorescein antibodies (Vector Laboratories, BA-0601, RRID:AB_2336069) followed by avidin-biotin complex (Vector Laboratories), TSA Biotin Tyramide Reagent (PerkinElmer), and Alexa488-conjugated streptavidin (Thermo Fisher Scientific). Fluorescent images were acquired with a TCS SP2 confocal microscope (Leica Microsystems). Brightness and contrast were linearly adjusted, and all adjustments were globally applied to confocal images and overlaid multiple fluorescence images using Photoshop (Adobe Systems). The presence of fluorescence signals was determined manually by visual inspection.

Table 1: Probes used for *in situ* hybridization analyses

Gene name	Accession no.	Probe region
Etv1	BC005645	1–2486
Tas1r1	AF337040	765–2761
Tas1r2	AF337041	641–2804
Tas1r3	AF337039	525–2725
Tas2r104	BC148229	1–921
Tas2r105	AF227147	1–903
Tas2r118	BC104401	1–900
Tas2r126	NM_207028	73–899
Scnn1a	BC133688	913–2333
Gnat3	AK040065	41–1019
Plcb2	BC145249	588–3123
Trpm5	AF228681	310–3491
Calhm1	LC270870	1–1407, 2148–2369
Calhm3	LC270871	1–1653
Pkd2l1	NM_181422	226–3275
Entpd2	NM_009849	20–1822

For double-fluorescence *in situ* hybridization in geniculate ganglia (GG), fluorescein-labeled probes and digoxigenin-labeled probes were sequentially detected as follows. Sections were incubated with biotin-conjugated anti-fluorescein antibodies, followed by avidin-biotin complex, TSA-plus Biotin solution (PerkinElmer), and Alexa488-conjugated streptavidin. After treatment with 3% H_2O_2 in PBS for 60 min, sections were then incubated with horseradish peroxidase-conjugated anti-digoxigenin antibodies (Roche, 11207733910, RRID:AB_514500) followed by TSA-plus Cyanine 3 solution (PerkinElmer) and 4',6-diamidino-2-phenylindole (DAPI). The fluorescent images were acquired, and optical confocal images were processed as described above. Only neurons whose profiles contain a nucleus with and without fluorescence signals were counted, and the frequencies of expression of *Etv1*-derived transcripts in *P2x2*$^+$ neurons and those of *P2x2*$^+$ neurons in GG were quantitatively analyzed using every 10 sections (i.e., 80 μm apart) of the GG of wild-type and *Etv1*$^{C/C}$ mice ($n = 3$ for each genotype).

Double labeling of *Scnn1a* with other genes with a combination of chromogenic and fluorescent signals was conducted as previously described (Taruno et al., 2013; Ohmoto et al., 2020a). The fluorescent signals were first developed using a biotin-conjugated anti-fluorescein antibody (Vector Laboratories) followed by avidin-biotin complex (Vector Laboratories), TSA Biotin Tyramide Reagent (PerkinElmer), and Alexa488-conjugated streptavidin (Thermo Fisher Scientific). After acquiring the fluorescent images, the chromogenic signals for *Scnn1a* were detected using an alkaline phosphatase-conjugated anti-digoxigenin antibody and 4-nitroblue tetrazolium chloride/5-bromo-4-chloro-3-indolyl-phosphate. The signals were developed for 7 d. Stained images were obtained as described above. Fluorescent and stained images were processed with Photoshop (Adobe Systems) and analyzed on a computer screen. Fluorescence signal and chromogenic stain surrounding a nucleus were counted as positive signal. Sporadic punctate fluorescence was regarded as nonspecific background. The frequencies of expression of *Scnn1a* in *Skn-1a*$^+$ cells (i.e., sodium taste cells) were semiquantitatively analyzed by calculating the ratios of

Table 2: Primers used for qPCR analyses

Gene	Accession no.	Amplified region	Forward primer (5′–>3′)	Reverse primer (5′–>3′)
Gapdh	BC085315	735–843	GCATGGCCTTCCGTGTTCCTA	GATGCCTGCTTCACCACCTTCT
Etv1	L10426	221–392	GCAAGTGCCTTACGTGGTCAC	AGGTACCTGAGCTTCAGCAAG
		1320–1517	CGTTGGGGCATTCAGAAGAAC	TTCCATGTCCGTCTTCAGCAG
Tas1r1	AF337040	1651–1795	ACAATCAGGTGCCTGTGTCAG	TGGCAGGTGTGAAGCTCACTC
Tas1r2	AF337041	1284–1446	TCGTCTATCCATGGCAGCTAC	TAGGAGGCGATGCTTTGGAAG
Tas1r3	AF337039	481–652	ACCTTCAACGGCACCCTTCAG	CAGGTGAAGTCATCTGGATGC
Gnat3	BC147839	530–679	GACTTAGACAGACTCACAGCC	CTCTGATCTCTGGCCACCTAC
Plcb2	NM_177568	1731–1857	CCTGGAGGTGACAGCTTATGA	GAGCTCCGTGAAGGAAGAGAC
Trpm5	AF228681	3320–3491	GGAAAACGGCACACAGAGTGG	CCACAGTTCTGAGAGCTTGAG
Calhm1	LC270870	535–665	TTGCGCTGCATCTCTCAGGCA	TAGTGGGACCAGTACTTGCTC
Calhm3	LC270871	453–571	GCAAGTGCAGCTCTTCCTAGC	TCCAGCCGATGGCCTGTGACA
Tas2r104	BC148229	488–635	ACATCCTGGCTGATCCACCTG	ATTGCATCTGCCTGCTGTGTC
Tas2r105	BC125541	160–318	TGACTGGCTTCCTTCTCATCG	TCAGGTGATTCACAGTCATCC
Tas2r118	BC104401	298–411	GCTGTCCTCTACTGTGTCAAG	AGAAGCTATCAGAGCACCCAG
Tas2r126	NM_207028	511–678	AAGGAGTGGAACAGAAGGCTG	GTTGGGGTCTTGCAAGCTGTG
Scnn1a	NM_011324	2107–2259	GTCTGTGAAGTCCCAGGATTG	ACCATCGTGACAGAGGGAGAC
Pkd2l1	NM_181422	1715–1921	TGCCATCGACAATGCCAACAG	CGCAGCCTTAGTAGGGTCTTG
Entpd2	NM_009849	395–560	CATGCGCCTACTCAACCTGAC	GTTCTCCAGCAGGTAGTTGGC

taste bud profiles that harbored at least one cell co-expressing *Skn-1a* and *Scnn1a* to all taste bud profiles using every 8 and 10 sections of palate and fungiform papillae (FuP), respectively, of wild-type and $Etv1^{C/C}$ mice ($n = 3$ for each genotype). $Scnn1a^{+}$ cells devoid of *Skn-1a* signal, which are likely sour taste cells (Chandrashekar et al., 2010; Ohmoto et al., 2020a), were not counted.

Quantitative PCR

Epithelia of CvP, anterior tongue, and soft palate, and DRG and GG were dissected from C57BL/6J mice and $Etv1^{C/C}$ mice. Total RNA was extracted using TRIzol (Life Technologies, 15596026), and cDNA was synthesized using SuperScript IV VILO Master Mix with ezDNase Enzyme (Life Technologies, 11766050). Quantitative PCR (qPCR) was performed using Fast SYBR Green Master Mix kit (Applied Biosystems, 4385612). Genes that did not show single peaks of melt curve in a C57BL/6J tissue were regarded as "not amplified" and removed from further analyses. *Gapdh* was used as a control to normalize the expression levels of individual genes. The relative gene expression level was calculated as $2^{-(CTTarget-CTGapdh)}$ (Livak and Schmittgen, 2001). Details about the primers used are given in Table 2.

5′-RACE

First strand cDNA to *Etv1* gene-derived transcript in the total RNA extracted from DRG of C57BL/6J mice was synthesized after the treatment with ezDNase Enzyme (Life Technologies, 11766050) using a primer 5′-TTCCATG TCCGTCTTCAGCAG-3′, which is also used to amplify C-terminal coding region of Etv1 by qPCR, and then polyadenylated by terminal deoxynucleotidyl transferase. A 5′ end of *Etv1* gene-derived transcript was amplified by PCR using a primer 7R1 (5′-CGGTCAGGTTTCGGAGTATGA GC-3′) and oligo(dT) primer and then a primer 7R2 (5′-ATAGTCGACCACTTGTGGCTTCTGATCATAGGC-3′) and oligo(dT) primer. Sequence of the amplified cDNA fragment was determined using the primer 7R2.

Immunohistochemistry

Immunohistochemical analyses using 4% PFA-fixed sections were conducted as previously described (Ohmoto et al., 2008). The sections were treated in a preheated target retrieval solution (pH 9; Agilent Technologies) at 80°C for 20 min before blocking. Primary antibodies used were rabbit anti-Etv1 (1:500, Abcam, ab81086, RRID:AB_1640495), rabbit anti-Trpm5 (1:3000, Alomone Labs, ACC-045, RRID:AB_2040252), mouse anti-IP_3R3 (1:1000, BD Biosciences, 610312, RRID:AB_397704), goat anti-KCNQ1 (1:300, Santa Cruz Biotechnology, sc-10646, RRID:AB_2131554), rabbit anti-Ddc (1:2000, GeneTex, GTX30448, RRID:AB_367199), goat anti-parvalbumin (1:500, Swant, PVG-213, RRID:AB_2650496), and rabbit anti-P2X2 (1:500, Sigma-Aldrich, P7982, RRID:AB_261187) antibodies. For single staining, signals were developed using a biotin-conjugated anti-rabbit IgG antibody (1:500, Vector Laboratories, BA-1000, RRID:AB_2313606) followed by avidin-biotin complex (Vector Laboratories) and the Metal Enhanced DAB Substrate kit (Thermo Fisher Scientific). For fluorescent labeling, Alexa 488-conjugated, 555-conjugated, and 647-conjugated antibodies [1:500, Thermo Fisher Scientific, A11029 (RRID:AB_138404), A11034 (RRID:AB_2576217), A11055 (RRID:AB_2534102), A21206 (RRID:AB_2535792), A21245 (RRID:AB_141775), A21432 (RRID:AB_2535853), A21447 (RRID:AB_141844)] were used as the secondary antibodies. Stained and fluorescent images were acquired and processed as described above.

Fluorescent labeling of KCNQ1 and double-fluorescence labeling of IP_3R3 and Ddc (also known as AADC) were conducted using every 12, 6, and 6, sections of CvP, FuP, and palate, respectively, of $Etv1^{C/+}$; $R26^{Tom/+}$ (heterozygous control) and $Etv1^{C/C+}$; $R26^{Tom/+}$ mice ($n = 3$ for each genotype). The sections were counterstained with DAPI, and fluorescent images were acquired with a confocal microscope. $KCNQ1^{+}$ cells, Ddc^{+} cells, IP_3R3^{+} cells, and IP_3R3^{+}tdTomato^{+} cells that had DAPI signals in taste bud profiles were counted, and the ratios of IP_3R3^{+}tdTomato^{+} cells to IP_3R3^{+} cells were calculated.

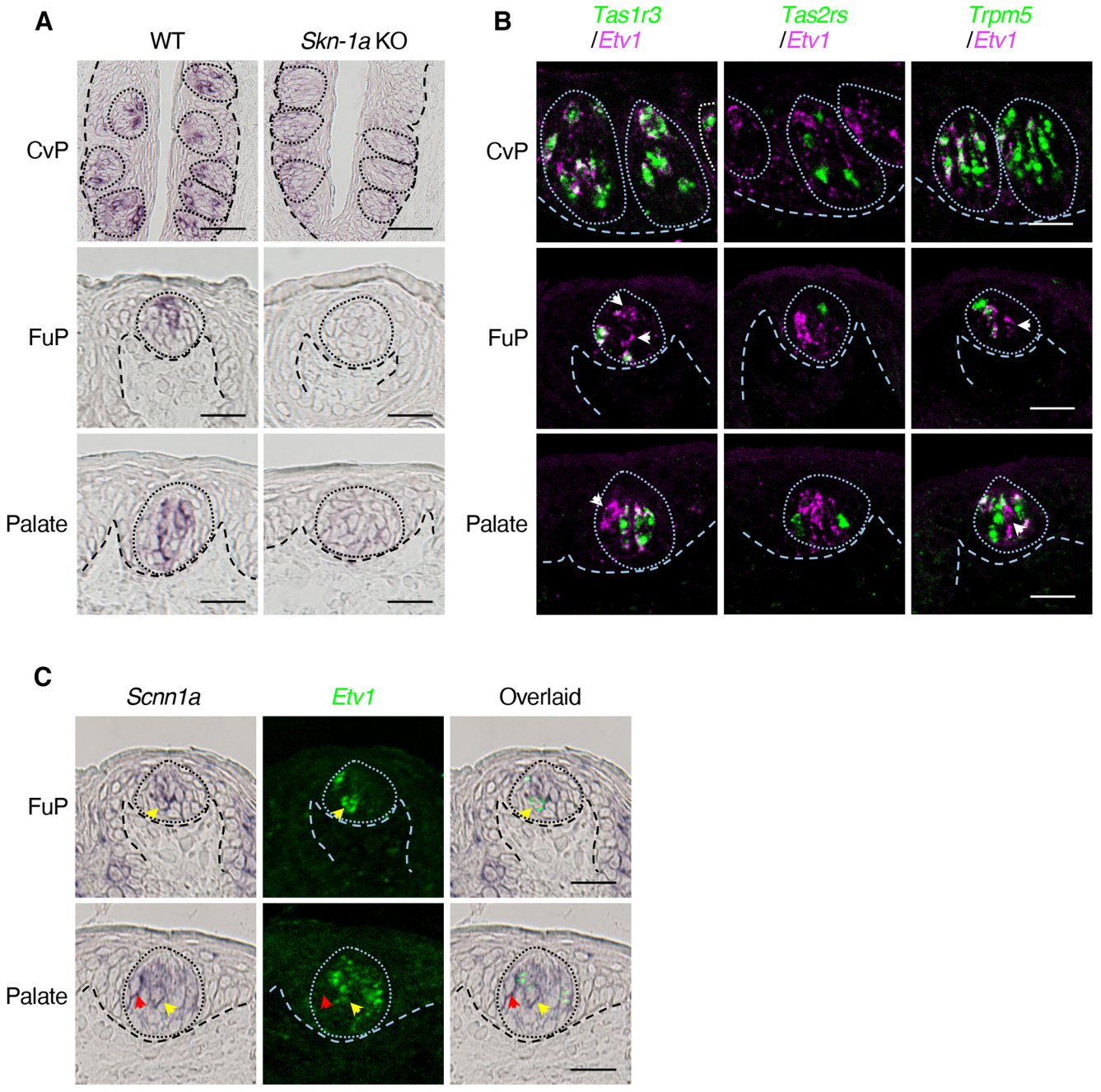

Figure 1. *Etv1* is expressed in a subset of Skn-1a-dependent taste cells. ***A***, Single-color *in situ* hybridization studies to investigate the expression of *Etv1* mRNA in taste buds in circumvallate (CvP; top) and fungiform (FuP; middle) papillae and in palate (bottom) of wild-type (WT; left) and *Skn-1a*$^{-/-}$ (right) mice. $n = 3$ for CvP, $n = 1$ for palate and FuP; $n \geq 9$ sections for each experiment. Scale bars: CvP, 50 μm; FuP and palate, 25 μm. ***B***, Double-fluorescence *in situ* hybridization of *Etv1* (magenta) with marker genes (green) in the CvP (top), FuP (middle), and palate (bottom) taste buds in WT mice. White arrowheads indicate cells singly expressing *Etv1*. For each experiment: CvP, $n \geq 2$, with ≥7 sections; FuP, $n \geq 2$, with ≥18 sections; palate, $n \geq 1$, with ≥9 sections. Scale bars: 25 μm. ***C***, Double-labeling *in situ* hybridization to study expression of *Scnn1a* in *Etv1*$^{+}$ taste cells: *Scnn1a* (dark purple; left), *Etv1* (green; middle), and merged (right) images of FuP (top) and palate (bottom) taste buds of WT mice. Yellow arrowheads indicate cells co-expressing *Scnn1a* and *Etv1*; red arrowheads indicate cells expressing only *Scnn1a*. $n = 3$ for each experiment. Scale bars: 25 μm. Taste buds and basal epithelial-mesenchymal boundaries are indicated by broken lines.

Double-fluorescence labeling of P2X2 and KCNQ1 was conducted in gustatory tissues of wild-type and *Etv1*$^{C/C}$ mice ($n = 2$ for each genotype). The sections were counterstained with DAPI, and fluorescent images were acquired with a confocal microscope in a Stellaris 5 WLL AOBS system (Leica Microsystems). Serial z-stacks were merged as maximum projection images using LASX software.

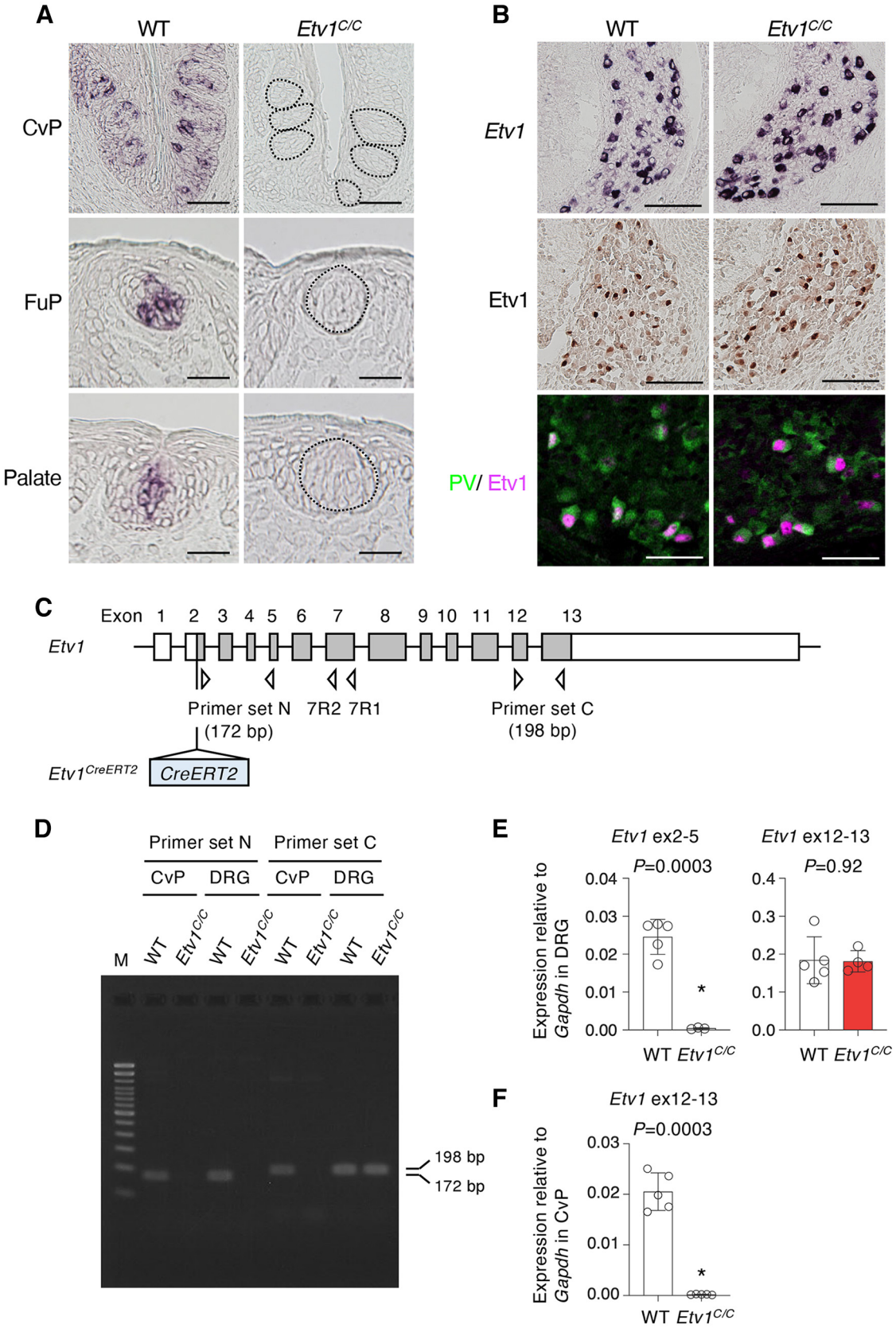

Figure 2. Loss of expression of *Etv1* mRNA in taste buds of *Etv1*$^{C/C}$ mice. ***A***, Single-color *in situ* hybridization studies to investigate the expression of *Etv1* mRNA in taste buds in circumvallate (CvP; top) and fungiform (FuP; middle) papillae and in palate (bottom) of wild-type (WT; left) control and *Etv1*$^{C/C}$ (right) mice. Taste buds in *Etv1*$^{C/C}$ mice are indicated by broken lines. $n = 3$ for CvP, $n = 1$ for

continued

FuP and palate; ≥9 sections for each experiment. Scale bars: CvP, 50 μm; FuP and palate, 25 μm. ***B***, Expression of mRNA (top) and protein (middle and bottom) of Etv1 isoform(s) in the sensory neurons in the dorsal root ganglia of wild-type (WT; left) and *Etv1*$^{C/C}$ (right) embryos at embryonic day 15.5. Etv1-immunoreactive signals (magenta) were observed in the parvalbumin (PV, green)-expressing proprioceptive neurons (bottom). $n = 3$ for each experiment, 10 sections for each genotype. Scale bars: 100 μm (chromogenic images) and 50 μm (fluorescent images). ***C***, Schematic structure of *Etv1* gene and its *CreERT2* knock-in allele. Boxes indicate exons. Protein coding regions are shaded. Primers used for PCR analyses are indicated by triangles (see Table 2). The reverse primer of the primer set C and primers 7R1 and 7R2 were used for 5'-RACE. *CreERT2* sequence is inserted in front of the forward primer of the primer set N in the second exon of *Etv1* (Extended Data Fig. 2-1). ***D***, Gel image of agarose electrophoresis of qualitative PCR products from circumvallate papillae (CvP) and dorsal root ganglia (DRG) of wild-type (WT) and *Etv1*$^{C/C}$ mice. Predicted amplicon sizes by primer sets N and C are 172 and 198 bp, spanning from exon 2 to exon 5 and from exon 12 to exon 13, respectively. Lane M, 100-bp DNA ladder marker. ***E***, ***F***, qPCR analyses to detect the expression of *Etv1* and/or *Etv1*-derived transcripts in DRG (***E***) and CvP (***F***) in WT and *Etv1*$^{C/C}$ mice. Open circles, individual data; white and red bars are the mean ± SD of WT and *Etv1*$^{C/C}$ mouse tissues, respectively. Significance was assessed by Welch's *t* test. Primers used are sets N and C to DRG (***E***) and set C to CvP (***F***). $n = 5$ for WT mice; $n = 4$ for DRG and $n = 5$ for CvP for *Etv1*$^{C/C}$ mice.

Whole chorda tympani nerve recordings

We investigated the electrophysiological response of the chorda tympani nerve in mice of the wild-type and *Etv1*$^{C/C}$ mice at two to four months old of both sexes ($n = 8$ per genotype). The experimenters were blinded to the genotype of the mice during testing. The mice were anesthetized with an intraperitoneal injection of a mixture of 4.28 mg/ml ketamine, 0.86 mg/ml xylazine, and 0.14 mg/ml acepromazine in saline (5 μl/g body weight). Anesthesia was maintained with additional injections. Each mouse was fixed with a head holder after its trachea was cannulated; then the chorda tympani nerve was dissected free from the lingual nerve near the tympanic bulla, cut, and placed on a platinum wire recording electrode. An indifferent electrode touched the walls of the wound. Taste stimuli were delivered to the tongue with a computer-controlled open flow system under constant flow and temperature (25°C) conditions. Each stimulation lasted for 30 s with a 60-s rinse between stimulations. Care was taken to ensure the flow was directed over the FuP. The nerve impulses were fed into a custom-made amplifier, monitored over a loudspeaker and with an oscilloscope, and recorded (PowerLab/sp4; AD Instruments). The integrated response during stimulation was calculated by subtracting the area of nerve activity preceding the stimulation from that during stimulation. Thus, the data reflect the level of activity during the stimulation period. The responses to all compounds were expressed relative to the response to 0.1 M NH_4Cl for each mouse. The averages for each animal and group were calculated for the statistical analyses.

Statistical analyses

Data are shown as the mean ± SD except those of gustatory nerve recordings that are shown as the mean ± SEM. A Welch's *t* test (for qPCR, taste bud numbers, taste bud cell populations, and tdTomato$^+$ cell ratio to IP_3R3^+ taste cell) or repeated-measures two-way ANOVA (for gustatory nerve recordings) was used to determine the effects of genotype using Prism 6 and 8 software (GraphPad Software). Sidak's multiple comparison tests were conducted to identify significant differences between pairs of mean values.

Results

Expression of *Etv1* in taste cells

We examined the expression of *Etv1* mRNA in mouse taste buds by *in situ* hybridization (for probe lengths and regions, see Table 1) and observed signals in a minor subset of taste bud cells in all gustatory areas of wild-type mice but not in *Skn-1a*-deficient mice, which indicates the restricted expression of *Etv1* mRNA in Skn-1a-dependent taste cells (Fig. 1*A*). Double-fluorescence *in situ* hybridization analyses showed that *Etv1* is expressed in a subset of *Skn-1a*$^+$ and *Trpm5*$^+$ (i.e., sweet, umami, and bitter taste) cells in the CvP in the wild-type mice, especially in *Tas1r3*$^+$ cells, but not in *Tas2r*$^+$ cells responsible for bitter taste (Fig. 1*B*). In taste buds in the FuP and palate, *Etv1* was present in the cells lacking *Tas1r3*, *Tas2r*, and *Trpm5* expression in addition to *Tas1r3*$^+$ cells, suggesting its expression in sodium-taste cells. Double-label *in situ* hybridization of *Etv1* with *Scnn1a* showed partial co-expression in taste cells in the FuP and palate (Fig. 1C). Together with its restricted expression to Skn-1a-dependent taste cells, these results indicate that *Etv1* is expressed in *Skn-1a*$^+$*Scnn1a*$^+$ sodium-taste cells (Ohmoto et al., 2020a). Therefore, gene expression analyses demonstrate that *Etv1* is expressed in sweet, umami, and sodium taste cells, all of which are involved in eliciting taste preferences.

Etv1 deficiency in taste buds of *Etv1*$^{C/C}$ mice

Mutant mouse strains with a null or loss-of-function mutation for Etv1 are useful models to study the function of Etv1 in the taste system. *Etv1*$^{C/C}$ mice are designed to encode a tamoxifen-inducible Cre recombinase (CreER) instead of Etv1 and carry a *CreERT2-frt* sequence in exon 2 in place of the initial ATG of the *Etv1* coding sequence (Extended Data Fig. 2-1*A*; Taniguchi et al., 2011). Therefore, they were expected to be conventional knock-outs like *Etv1*^{nlslacZ} mice (Extended Data Fig. 2-1*A*; Arber et al., 2000). *Etv1*$^{C/C}$ mice, however, are viable and fertile and do not present any overt abnormalities, although other Etv1-null mutant strains (*Etv1*$^{ETS/ETS}$ and *Etv1*$^{nlslacZ/nlslacZ}$ mice; for their allele structures, see Extended Data Fig. 2-1*A*) exhibit limb ataxia or abnormal postures attributable to defects in proprioceptive function and die three to five weeks after birth (Arber et al., 2000; Patel et al., 2003). Therefore, we first

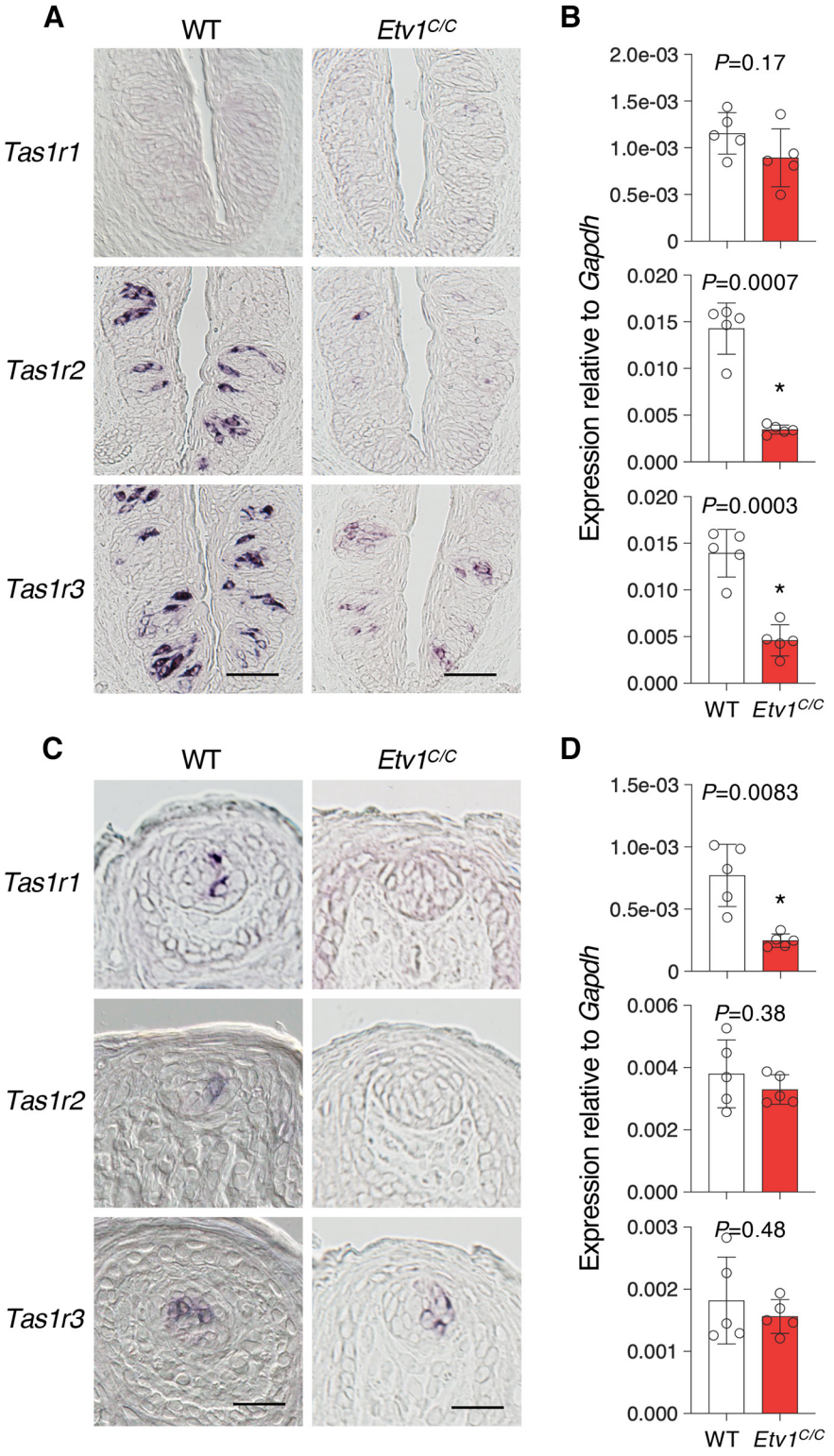

Figure 3. Etv1 regulates the expression of T1R genes in taste cells. The expression of T1R taste receptor genes in taste buds was analyzed in circumvallate (***A***, ***B***) and fungiform (***C***, ***D***) papillae and soft palate (Extended Data Fig. 3-1) of wild-type (WT) and *Etv1*$^{C/C}$ mice. ***A***, ***C***, *In situ* hybridization analyses. Left, WT mice ($n = 3$; ≥9 sections for CvP, ≥27 sections for FuP). Right, *Etv1*$^{C/C}$ mice ($n = 3$; ≥9 sections for CvP, ≥27 sections for FuP). Scale bars: CvP, 50 μm and FuP, 25 μm. ***B***, ***D***, qPCR analyses. $n = 5$ for each genotype. Open circles, individual data; white and red bars are the mean ± SD of WT and *Etv1*$^{C/C}$ tissues, respectively. Significance was assessed by Welch's *t* test.

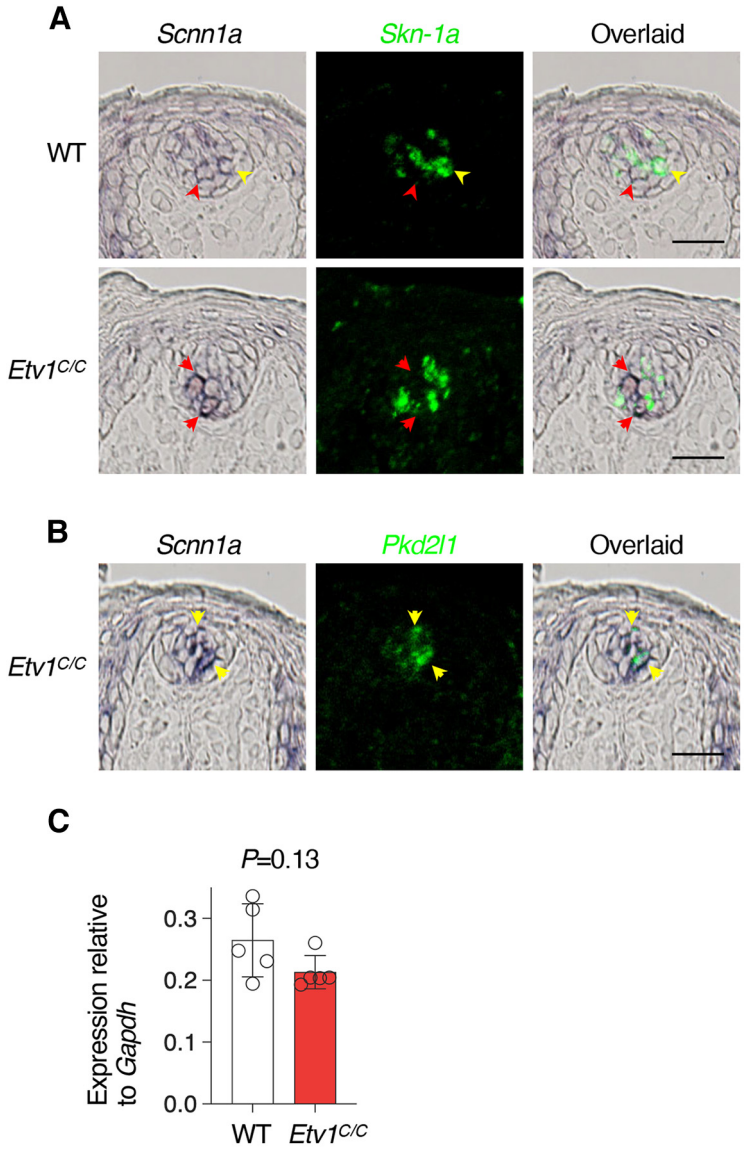

Figure 4. Etv1 positively regulates expression of the *Scnn1a* sodium taste receptor gene. ***A***, ***B***, Double-label *in situ* hybridization demonstrates expression of *Scnn1a* in *Skn-1a*$^+$ taste cells (***A***) and in *Pkd2l1*$^+$ taste cells (***B***). Shown are *Scnn1a* (dark purple; left), *Skn-1a* or *Pkd2l1* (green; middle), and overlaid (right) images of taste buds in fungiform papilla of wild-type (WT) and *Etv1*$^{C/C}$ mice. Yellow arrowheads indicate cells co-expressing *Scnn1a* with *Skn-1a* (***A***) or *Pkd2l1* (***B***), and red arrowheads indicate cells expressing only *Scnn1a*. $n = 3$; 27 sections for each genotype (***A***); $n = 2$; 18 sections (***B***). Scale bars: 25 μm. ***C***, qPCR analysis of *Scnn1a* in taste buds in fungiform papillae of WT and *Etv1*$^{C/C}$ mice. $n = 5$ for each genotype. Open circles, individual data; white and red bars are the mean ± SD of WT and *Etv1*$^{C/C}$ tissues, respectively. Significance was assessed by Welch's *t* test.

evaluated whether *Etv1* is knocked out in *Etv1*$^{C/C}$ mice. *Etv1* mRNA was completely absent in taste buds in all gustatory areas examined in *Etv1*$^{C/C}$ mice, while taste buds of wild-type mice showed *Etv1* mRNA signals (Fig. 2*A*). Intriguingly, however, we observed the signals of *Etv1* mRNA and protein in a subset of dorsal root ganglia (DRG) neurons of wild-type and *Etv1*$^{C/C}$ mice (Fig. 2*B*); the frequency and intensity of these signals in *Etv1*$^{C/C}$ mice were qualitatively comparable to those in wild-type mice. Etv1 immunoreactivity was observed in most parvalbumin$^+$ neurons (i.e., proprioceptive sensory neurons) in both wild-type and *Etv1*$^{C/C}$ mice (Fig. 2*B*). These results indicate that the *Etv1*$^{C/C}$ mice are Etv1 null mutant in taste buds and suggest that Etv1 variant(s) are expressed in DRG neurons.

To determine whether Etv1 is knocked out and whether an Etv1 variant is expressed in DRG of *Etv1*$^{C/C}$ mice, we performed qualitative PCR and qPCR using primers corresponding to N-terminal and C-terminal coding sequences. cDNA fragments corresponding to N-terminal coding sequence were not amplified from CvP or DRG of *Etv1*$^{C/C}$ mice, indicating the disruption of *Etv1* by the insertion of *CreERT2* in DRG as well as CvP (Fig. 2*C–F*; Extended Data Fig. 2-1). However, cDNA fragments corresponding to the ETS domain in the C-terminal region were amplified from DRG but not from CvP of *Etv1*$^{C/C}$ mice (Fig.

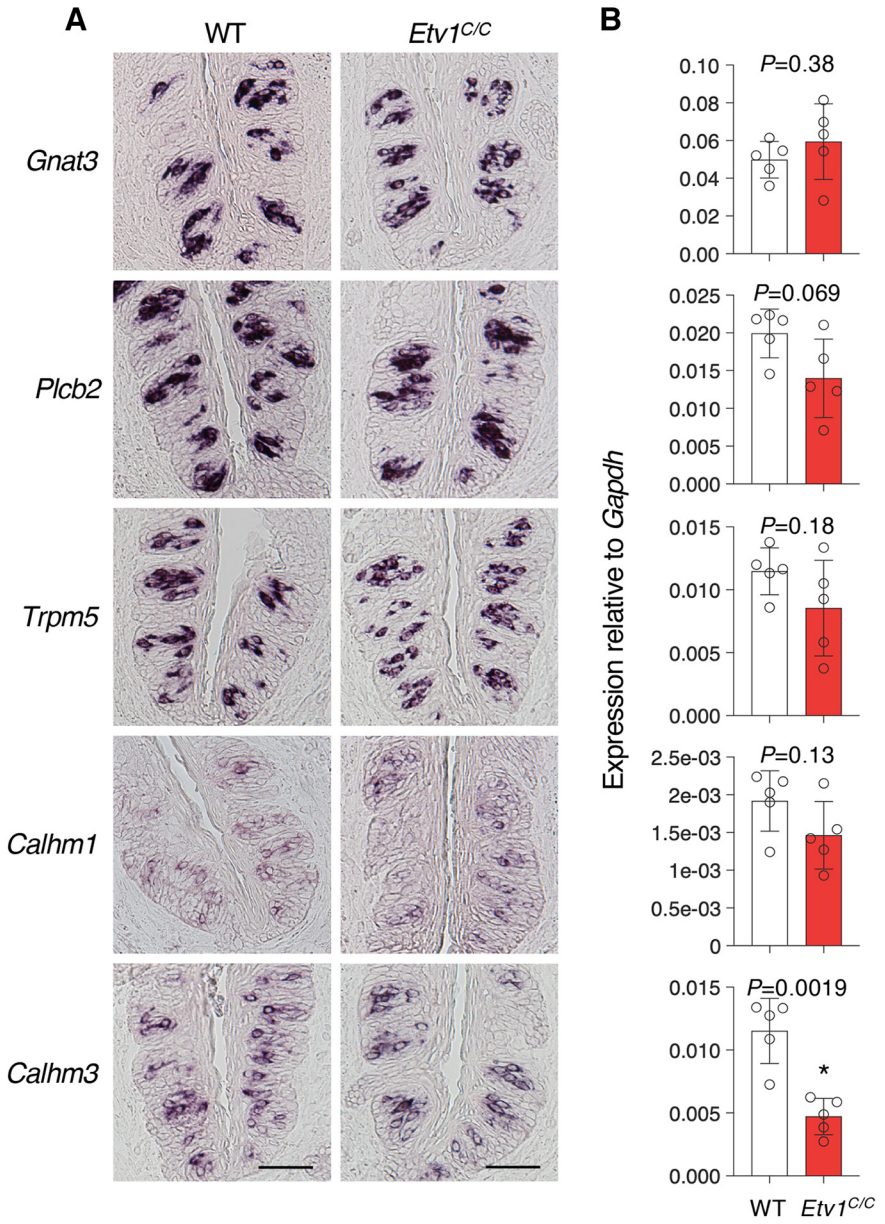

Figure 5. Limited impact of *Etv1* deficiency on expression of taste signaling genes necessary for T1R-mediated tastes. ***A***, Expression of *Gnat3*, *Plcb2*, *Trpm5*, *Calhm1*, and *Calhm3* that are partially co-expressed with *Etv1* in circumvallate papillae of wild-type (WT; left) and $Etv1^{C/C}$ (right) mice by *in situ* hybridization. $n = 1$ for each genotype, for each experiment; 3 sections. Scale bars: 50 μm. ***B***, qPCR analyses in taste buds in circumvallate papillae of WT and $Etv1^{C/C}$ mice. $n = 5$ for each genotype. Open circles, individual data; white and red bars are the mean ± SD of WT and $Etv1^{C/C}$ tissues, respectively. Significance was assessed by Welch's *t* test. For results in fungiform papillae and soft palate, see Extended Data Figures 5-1 and 5-2, respectively.

2*C*–*F*; Extended Data Fig. 2-1*A*). 5'-RACE revealed that a major transcript in DRG is *Etv1* variant 2 (*Etv1*-v2, NM_001163154), which has little impact of its expression by CreERT2 insertion (Fig. 2*C*; Extended Data Fig. 2-1*B*,*C*). These results indicate that the $Etv1^{C/C}$ mice are Etv1 null mutant in taste buds and that the major transcript from the *Etv1* allele in taste tissues is *Etv1*. In DRG, *Etv1*-v2 and its encoded protein, Etv1 isoform b, are expressed in DRG neurons, in addition to Etv1 mRNA and protein, in proprioceptive neurons. It remains unclear whether the Etv1 isoform b is as functional as Etv1, although it can seemingly compensate for the loss of Etv1 in the proprioceptive neurons.

Involvement of Etv1 in the expression of taste receptor genes in $Etv1^{+}$ cells in taste buds

To understand the role of Etv1 in taste cells, we studied the impact of *Etv1* deficiency on taste receptor gene expression by *in situ* hybridization and qPCR analyses in taste buds of $Etv1^{C/C}$ mice. The umami taste receptor gene *Tas1r1*, which is predominantly expressed in the taste buds in FuP and palate but rarely detected in CvP of

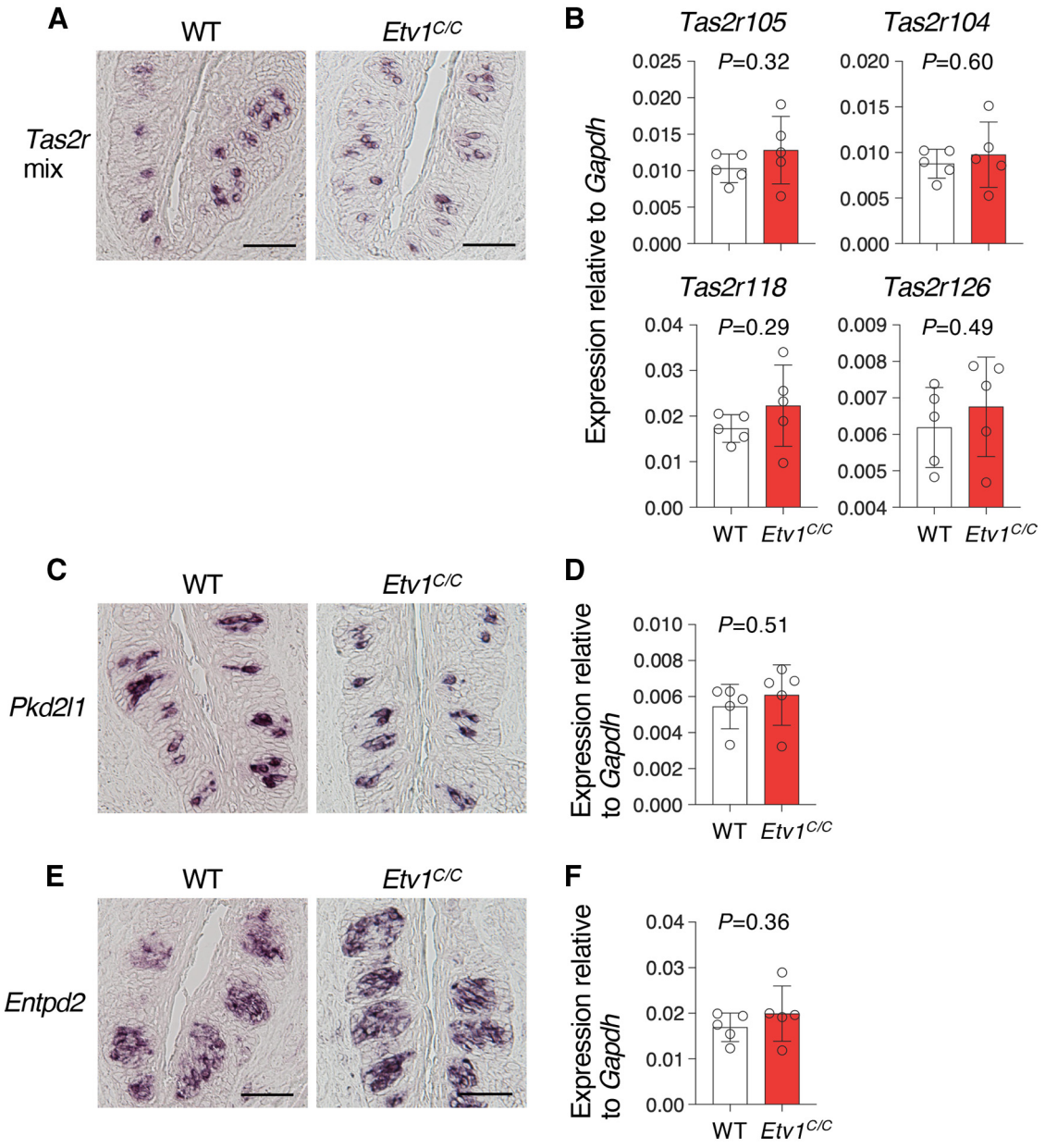

Figure 6. Unaltered expression of genes that are not co-expressed with *Etv1* by *Etv1* deficiency. Expression of T2R genes, *Pkd2l1*, and *Entpd2* was examined in circumvallate papillae of wild-type (WT) and $Etv1^{C/C}$ mice. ***A***, ***C***, ***E***, *In situ* hybridization. T2R gene expression was examined using a mixture of probes to four T2R genes (*Tas2r104*, *Tas2r105*, *Tas2r118*, and *Tas2r126*). Left, WT. Right, $Etv1^{C/C}$ mice. For each genotype, $n = 2$, with 5 sections for T2R genes; $n = 1$, with 3 sections for *Pkd2l1* and *Entpd2*. Scale bars: 50 μm. ***B***, ***D***, ***F***, qPCR analyses. T2R genes used for *in situ* hybridization were individually measured (***B***). $n = 5$ for each genotype. Open circles, individual data; white and red bars are the mean ± SD of WT and $Etv1^{C/C}$ tissues, respectively. Significance was assessed by Welch's *t* test. For results in fungiform papillae and soft palate, see Extended Data Figures 6-1 and 6-2, respectively.

wild-type mice, as reported previously (Hoon et al., 1999; Nelson et al., 2001), was completely absent from the taste buds of any gustatory area of $Etv1^{C/C}$ mice (Fig. 3*A*,*C*; Extended Data Fig. 3-1*A*). The sweet taste receptor gene *Tas1r2*, which is predominantly expressed in the taste buds in CvP and palate but rarely detected in FuP of wild-type mice, as reported previously (Hoon et al., 1999; Nelson et al., 2001), was almost (in CvP) or completely (in FuP and palate) lost in taste buds of $Etv1^{C/C}$ mice (Fig. 3*A*,*C*; Extended Data Fig. 3-1*A*). qPCR analyses exhibited results consistent with *in situ* hybridization analyses but found no significant differences where *Tas1r1* and *Tas1r2* are rarely expressed in wild-type mice (Fig. 3*B*,*D*; Extended Data Fig. 3-1*B*). The sweet and umami taste receptor gene *Tas1r3* was less influenced by *Etv1* deficiency than were *Tas1r1* and *Tas1r2*: intensity and frequency of signals of *Tas1r3* in taste buds were weaker and sparser, respectively, than in

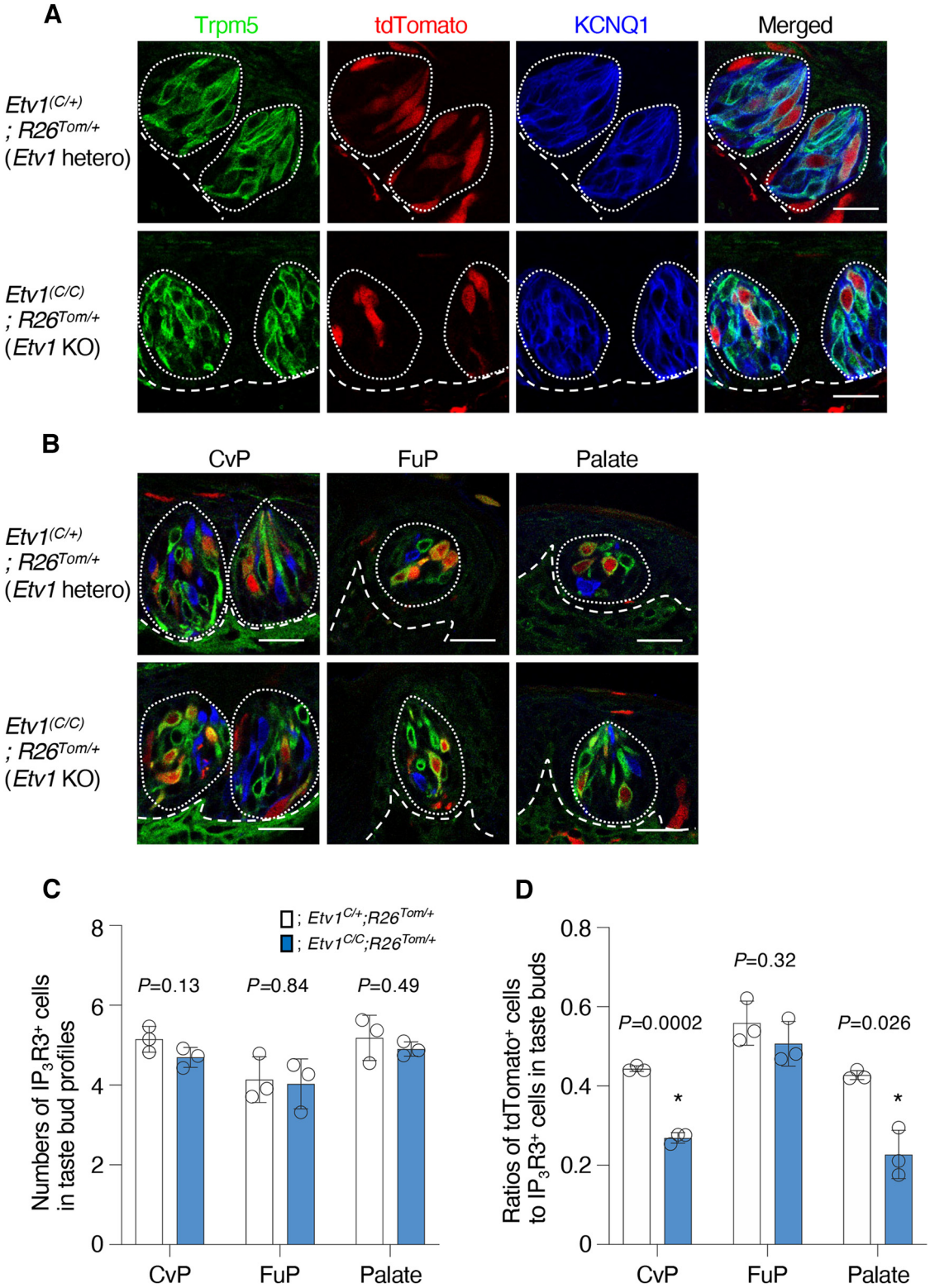

Figure 7. Presence of CreER^{+} taste cells in *Etv1*-deficient taste buds. ***A***, Triple-fluorescence labeling to study the impact of an *Etv1* deficiency on the generation of *Etv1*$^{+}$ taste cells in circumvallate papillae: Trpm5 (green; left) to identify Skn-1a-dependent taste cells, tdTomato (red; left middle) to identify *Etv1*$^{+}$ taste cells, KCNQ1 (blue; right middle) that marks most taste bud cells, and merged images (right) of circumvallate taste buds of *Etv1*$^{C/+}$; *R26*$^{Tom/+}$ (top) and *Etv1*$^{C/C}$; *R26*$^{Tom/+}$ (bottom) mice. $n = 2$, with 6 sections for each experiment. ***B***, Triple-fluorescence images for IP$_3$R3 (to identify Skn-1a-dependent taste cells, green) and tdTomato (to identify *Etv1*$^{+}$ taste cells, red), and Ddc (to identify sour taste cells, blue) in taste buds in circumvallate (CvP; left) and fungiform (FuP; center) papillae and palate (right) of *Etv1*$^{C/+}$; *R26*$^{Tom/+}$ (top) and *Etv1*$^{C/C}$; *R26*$^{Tom/+}$ (bottom) mice ($n = 3$ for each genotype).

continued

Taste buds and basal epithelial-mesenchymal boundaries are indicated by broken lines. Scale bars: 25 μm. ***C***, ***D***, Quantitative analyses of taste cell populations. The number of Skn-1a-dependent taste cells (***C***) and ratios of tdTomato$^+$ cells to Skn-1a-dependent taste cells (***D***) in single taste bud profiles in the CvP, FuP, and palate were compared between *Etv1*$^{C/+}$; *R26*$^{Tom/+}$ (white bar) and *Etv1*$^{C/C}$; *R26*$^{Tom/+}$ (blue bar) mice. Data are expressed as the mean ± SD. Significance was assessed by Welch's *t* test. For the populations of total taste bud cells and sour taste cells in single taste bud profiles, see Extended Data Figure 7-1.

wild-type mice (Fig. 3*A*,*C*; Extended Data Fig. 3-1*A*). qPCR showed drastic decrease in *Tas1r3* expression only in CvP of *Etv1*$^{C/C}$ mice (Fig. 3*B*,*D*; Extended Data Fig. 3-1*B*). However, *Tas1r3* signals were barely detectable in the taste buds in FuP and palate of *Etv1*$^{C/C}$ mice when signal was developed for a shorter time (Extended Data Fig. 3-1*C*,*D*), suggesting a decrease in *Tas1r3* expression by *Etv1* deficiency.

Scnn1a, a gene responsible for amiloride-sensitive salty taste, is expressed in all *Pkd2l1*$^+$ cells and a subset of *Skn-1a*$^+$ cells in taste buds in the FuP in wild-type mice, as reported previously (Chandrashekar et al., 2010; Ohmoto et al., 2020a). In *Etv1*$^{C/C}$ mice, *Scnn1a* was rarely co-expressed with *Skn-1a* in *Etv1*$^{C/C}$ mice (Fig. 4*A*), while its co-expression with *Pkd2l1*$^+$ in sour taste cells was unaltered (Fig. 4*B*), indicating that Etv1 is required for the *Scnn1a* expression in sodium taste cells. However, qPCR analyses exhibited higher relative expression of *Scnn1a* than of T1R genes in FuP and did not show significant differences between wild-type and *Etv1*$^{C/C}$ mice (Fig. 4*C*). *Scnn1a* may be expressed in many cells inside and/or outside taste buds at lower levels than in sour and sodium taste cells, and thus the decrease in sodium taste cells by *Etv1* deficiency may be too small to affect the total amount of *Scnn1a* detected by qPCR.

Next, we studied the impact of *Etv1* deficiency on the expression of genes encoding the downstream signaling molecules commonly required for sweet, umami, and bitter tastes. *In situ* hybridization analyses showed no obvious differences in the expression of any genes for taste signaling molecules between wild-type and *Etv1*$^{C/C}$ mice (Fig. 5*A*; Extended Data Figs. 5-1*A*, 5-2*A*). However, *Calhm3* expression was significantly decreased by *Etv1* deficiency in all gustatory areas examined, and the expression of *Calhm1* and *Plcb2* was also significantly decreased in one or two gustatory area (Fig. 5*B*; Extended Data Figs. 5-1*B*, 5-2*B*). Although it seems to be largely dispensable for the expression of taste signaling molecule genes, Etv1 may participate in their expression.

We then examined the expression of genes that in wild-type mice are expressed in *Etv1*-negative taste bud cells. Frequency of signals to T2R genes in taste buds of *Etv1*$^{C/C}$ mice were comparable to those in wild-type mice by *in situ* hybridization (Fig. 6*A*; Extended Data Figs. 6-1*A*, 6-2*A*). Consistent with this, qPCR analyses showed no significant difference between wild-type and *Etv1*$^{C/C}$ mice in CvP and FuP (Fig. 6*B*; Extended Data Fig. 6-1*B*). Intriguingly, however, the expression of three out of four T2R genes examined was significantly increased in palate (Extended Data Fig. 6-2*B*). The expression of *Pkd2l1* and the nonsensory taste bud cell marker *Entpd2* were also unaltered in the taste buds of *Etv1*$^{C/C}$ mice compared with wild-type mice (Fig. 6*C*–*F*; Extended Data Figs. 6-1*C*–*E*, 6-2*C*–*E*).

Collectively, these results suggest that Etv1 is involved in the differentiation of taste cells by regulating expression of taste receptor and taste signaling molecule genes in sweet, umami, and sodium taste cells.

Differential impact of *Etv1* deficiency on the composition of CreER$^+$ taste cells

The residual expression of T1R genes in the *Etv1*-deficient mice indicates that Etv1 is not indispensable for the generation of taste cells. To evaluate whether *Etv1* deficiency influences *Etv1*$^+$ taste cell populations, we generated *Etv1*$^{C/C}$; *R26*$^{Tom/+}$ mice (in which tdTomato expression is activated in *Etv1*$^+$ cells by tamoxifen injection) and examined whether tdTomato expression was observed in taste buds. In all gustatory areas examined, tdTomato expression was observed in a subset of taste bud cells of *Etv1*$^{C/C}$; *R26*$^{Tom/+}$ mice (Fig. 7*A*,*B*). Presence of tdTomato in taste buds of *Etv1*$^{C/C}$; *R26*$^{Tom/+}$ mice suggests that *Etv1* deficiency is not crucial for generation or maintenance of taste cells (Fig. 7*A*,*B*). We then identified Skn-1a-dependent taste cells using specific marker IP$_3$R3; distinguished *Etv1*$^+$ and *Etv1*$^-$ taste cells in Skn-1a-dependent cells as tdTomato$^+$ and tdTomato$^-$ cells, respectively; identified sour taste cells by the expression of sour taste cell marker Ddc; and calculated their number in single taste buds. The population of tdTomato$^+$ cells was significantly decreased to about half in CvP and palate of *Etv1*$^{C/C}$; *R26*$^{Tom/+}$ mice compared with that in the *Etv1*$^{C/+}$; *R26*$^{Tom/+}$ heterozygous control mice, while the populations of KCNQ1$^+$, Ddc$^+$, and IP$_3$R3$^+$ cells were unaltered in any gustatory areas (Fig. 7*C*,*D*; Extended Data Fig. 7-1). Intriguingly, no significant difference in the population of tdTomato$^+$ cells was observed in FuP between *Etv1*$^{C/C}$; *R26*$^{Tom/+}$ and *Etv1*$^{C/+}$; *R26*$^{Tom/+}$ heterozygous control mice (Fig. 7*B*,*C*). These results suggest that Etv1 is involved in generation and/or maintenance of taste cells. In CvP, the impact on the population of tdTomato$^+$ cells by *Etv1* deficiency is less pronounced than that on gene expression, and the expression of T2R genes is not increased (Fig. 6). Although we cannot completely preclude the increase of bitter taste cells and the involvement of Etv1 in cell fate choice toward sweet, umami, or sodium taste cells over bitter taste cells, the decrease of tdTomato$^+$ cells (and thus the increase of tdTomato$^-$ cells) seems to be simply explained by the decrease of CreER expression from *Etv1* gene: Etv1 may be involved in the positive-feedback regulation of *Etv1* gene expression in taste cells.

Etv1 expression in the cranial sensory neurons

Axotomy of gustatory nerves results in degeneration of taste cells (Guth, 1957; Kennedy, 1972; John et al., 2003; Guagliardo and Hill, 2007; Takeda et al., 2013).

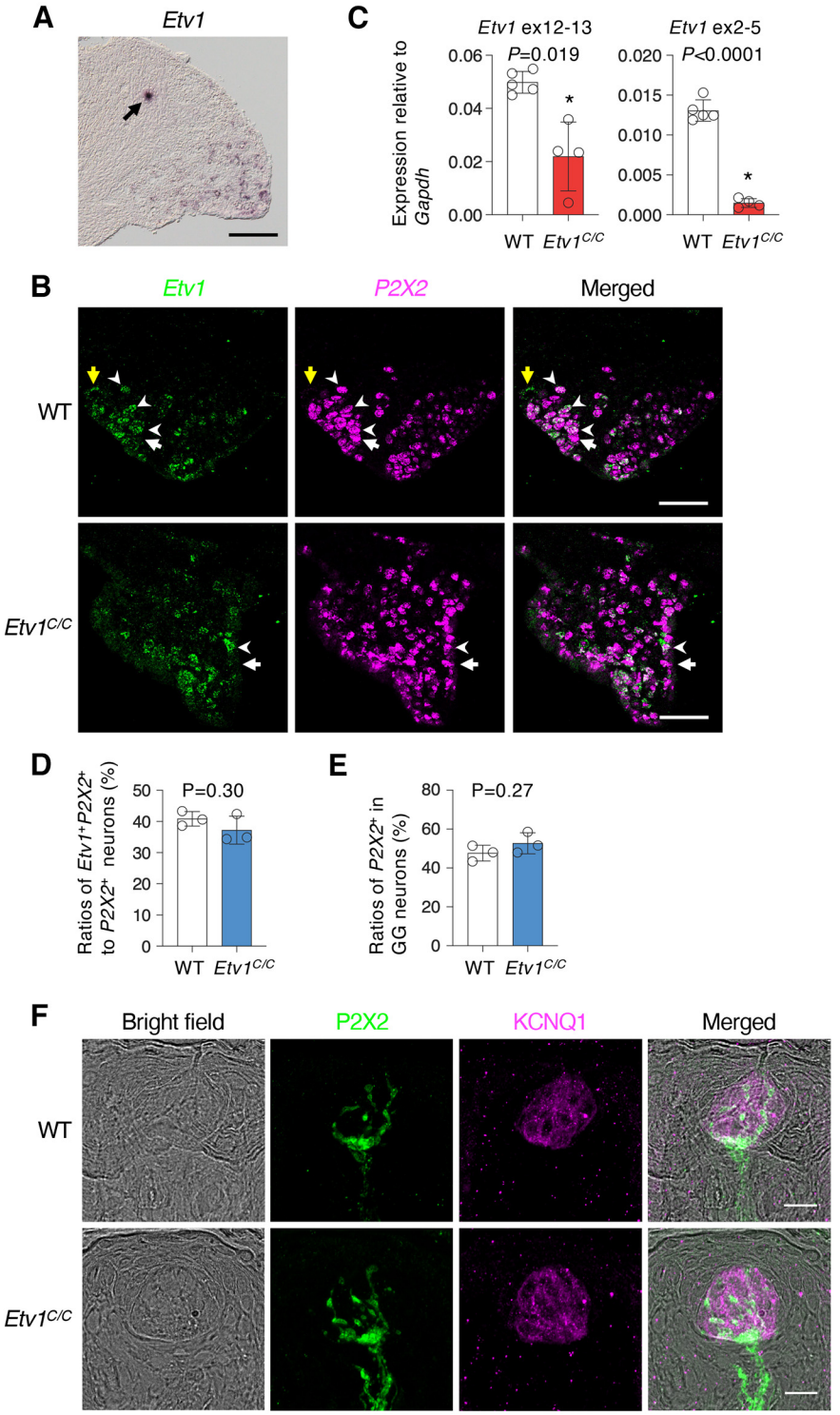

Figure 8. Expression of *Etv1*-related transcripts in geniculate ganglion neurons. ***A***, *In situ* hybridization to show the expression of *Etv1* and/or *Etv1*-related transcripts in geniculate ganglia of wild-type mice. Black arrow indicates nonspecific staining in the trunk of facial nerve. Scale bar: 100 μm. ***B***, Double-label *in situ* hybridization to study expression of *P2x2* in *Etv1*$^{+}$ neurons: *Etv1* (green; left), *P2x2* (magenta; middle), and merged (right) images of geniculate ganglia in wild-type (WT; top) and *Etv1*$^{C/C}$ (bottom) mice. White arrowheads, *Etv1*$^{+}$*P2x2*$^{+}$ neurons; white arrows, *Etv1*$^{-}$*P2x2*$^{+}$ neurons; and yellow arrows, *Etv1*$^{+}$*P2x2*$^{-}$ neurons. Scale bars: 100 μm. ***C***, qPCR analyses to detect the expression of *Etv1* and/or *Etv1*-related transcripts in geniculate ganglia. Primers used are sets N and C (for details, see Fig. 2C; Table 2). $n = 5$ for WT; $n = 4$ for *Etv1*$^{C/C}$ mice. ***D***, ***E***, Ratio of *Etv1*$^{+}$*P2x2*$^{+}$ neurons to *P2x2*$^{+}$ neurons (***D***) and ratio of *P2x2*$^{+}$ neurons to total neurons (***E***) in geniculate ganglia in WT and *Etv1*$^{C/C}$ mice. $n = 3$ for each genotype. Data are expressed as the mean ± SD. Significance was assessed by Welch's *t* test. ***F***, P2X2-immunoreactive fiber projection into taste buds in fungiform papillae: bright field (left), P2X2 (green; left middle), KCNQ1 (magenta; right middle), and merged images

continued
(right) of fungiform papillae of WT (top) and *Etv1*$^{C/C}$ (bottom) mice. Fluorescent images of P2X2$^+$ signals were merged images of serial z-stacks. $n = 2$, with 3–4 sections for each genotype. Scale bars: 20 μm. For results in circumvallate papillae and soft palate, see Extended Data Figure 8-1.

To evaluate whether the decrease of *Etv1*$^+$ taste cells in *Etv1*$^{C/C}$ mice is a cell-autonomous effect or a noncell-autonomous effect caused by the loss of gustatory neurons, we interrogated whether *Etv1* is expressed in sensory neurons in geniculate ganglia (GG) and, if it is expressed, whether *Etv1* is required for their generation and/or innervation. *In situ* hybridization yielded moderate signals in GG neurons in wild-type mice (Fig. 8*A*), predominantly in a minor subset of gustatory neurons expressing *P2x2* (Finger et al., 2005; Dvoryanchikov et al., 2017; Fig. 8*B*). Although qPCR showed little expression of *Etv1*, *Etv1*-derived transcripts putatively encoding Etv1 isoforms were amplified in GG in *Etv1*$^{C/C}$ mice (Fig. 8*C*). Consistently, signals of *Etv1*-derived transcripts were observed in *P2x2*-expressing GG neurons in *Etv1*$^{C/C}$ mice by *in situ* hybridization (Fig. 8*B*). Importantly, the ratios of *Etv1*$^+$*P2x2*$^+$ neurons to *P2x2*$^+$ neurons and *P2x2*$^+$ neurons to all GG neurons are comparable between *Etv1*$^{C/C}$ and wild-type mice (Fig. 8*D*,*E*). P2X2$^+$ fibers also comparably projected to taste buds, but not to surrounding epithelium devoid of anti-KCNQ1 antibody immunoreactivity, from mesenchymal tissues in both wild-type and *Etv1*$^{C/C}$ mice (Fig. 8*F*; Extended Data Fig. 8-1). Etv1 and its isoform(s) appear to be dispensable for the generation and survival of putative gustatory neurons.

Taste responsiveness of gustatory nerves by *Etv1* deficiency

Lastly, we examined electrophysiological responses to various taste substances from chorda tympani nerves that innervate taste cells in the FuP (Fig. 9*A*). Chorda tympani nerve responses to sucrose were significantly reduced but still observed in the *Etv1*$^{C/C}$ mice, and a greater reduction in responses to artificial sweeteners was observed (Fig. 9*B*; Table 3). *Etv1*$^{C/C}$ mice exhibited decreased chorda tympani nerve responses to inosine monophosphate and monosodium glutamate, but their synergistic effects were not observed: the responses of MSG+IMP are comparable to the sums of individual responses of MSG and IMP in *Etv1*$^{C/C}$ mice (Fig. 9*C*; Table 3). *Etv1*$^{C/C}$ mice showed severely reduced chorda tympani nerve responses to sodium chloride (NaCl) and no amiloride-sensitive components of the nerve responses to NaCl, while the amiloride-insensitive components remained almost normal (Fig. 9*D*; Table 3). We observed no significant changes in chorda tympani nerve responses to chemicals with a bitter or sour taste in the *Etv1*$^{C/C}$ mice (Fig. 9*E*,*F*; Table 3). These results of chorda tympani nerve recordings are well consistent with those of gene expression analyses in FuP. Together with the unaltered populations of putative gustatory neurons in GG and *Etv1*$^+$ taste cells in FuP, it is likely that gustatory neurons innervate taste cells in FuP in *Etv1*$^{C/C}$ mice and that the altered gene expression in *Etv1*$^+$ taste cells in *Etv1*$^{C/C}$ mice is a cell-autonomous effect of *Etv1* deficiency in taste cells. The decreased responses of chorda tympani nerves to sweet, umami, and sodium taste substances in *Etv1*$^{C/C}$ mice should thus be functional consequences of the diminished expression of T1R genes and *Scnn1a* because of *Etv1* deficiency in taste cells.

Discussion

Continuous normal turnover of taste cells underlies homeostasis of the sense of taste. Single stem cells can give rise to any type of taste bud cell (Ren et al., 2014), but the molecular mechanisms that generate specific individual taste bud cells remain poorly understood. This study revealed that *Etv1* participates in the differentiation of Skn-1a-dependent sweet, umami, and sodium taste cells by regulating the expression of taste receptor genes in them. Etv1 may be a part of the mechanism that, among Skn-1a-dependent cells, distinguishes sweet, umami, and sodium taste cells from bitter taste cells.

Differentiation of taste cells

Etv1 is expressed in sweet, umami, and sodium taste cells, and its deficiency impaired expression of genes encoding taste receptors and intracellular signal transduction molecules necessary for sweet, umami, and sodium tastes. Therefore, Etv1 appears to be involved in the differentiation of these taste cells in multiple ways. However, *Etv1* deficiency does not completely abolish the expression of taste receptor genes. There may be other molecules that are functionally redundant to Etv1 and may have partially compensated for the loss of Etv1 in taste cells in *Etv1*$^{C/C}$ mice; for example, Etv6 is expressed in *Tas1r3*$^+$ taste cells (Lee et al., 2017; Sukumaran et al., 2017). We presume that transcription factors specific to sweet, umami, and sodium taste cells, respectively, are expressed to characterize individual taste cell subsets and may compensate for Etv1 function to some extent in *Etv1*$^{C/C}$ mice, which explains the differential impacts of *Etv1* deficiency on gene expression. However, this hypothesis cannot fully explain regional differences in gene expression in specific taste cell subsets (e.g., *Tas1r2* expression in sweet taste cells in FuP and palate but not in CvP) or the effects on the composition of Skn-1a-dependent taste cells by *Etv1* deficiency. There may be more varieties of transcription factors in taste cells and more molecular mechanisms to generate such varieties than we understand today.

Expression of *Etv1* and *Eya1* seems to be reversely correlated in *Skn-1a*$^+$ cells in taste buds: *Eya1* is expressed in the putative precursor and bitter taste cells (Ohmoto et al., 2021), while *Etv1* is expressed in the remaining *Skn-1a*$^+$ cell types. In addition to its functions as a positive regulator of gene expression, Etv1 may negatively regulate T2R genes as a repressor in sweet, umami, and sodium taste cells. Partially consistent with this possibility, the expression of three out of four T2R genes examined was increased only in palate of the *Etv1*$^{C/C}$ mice. This

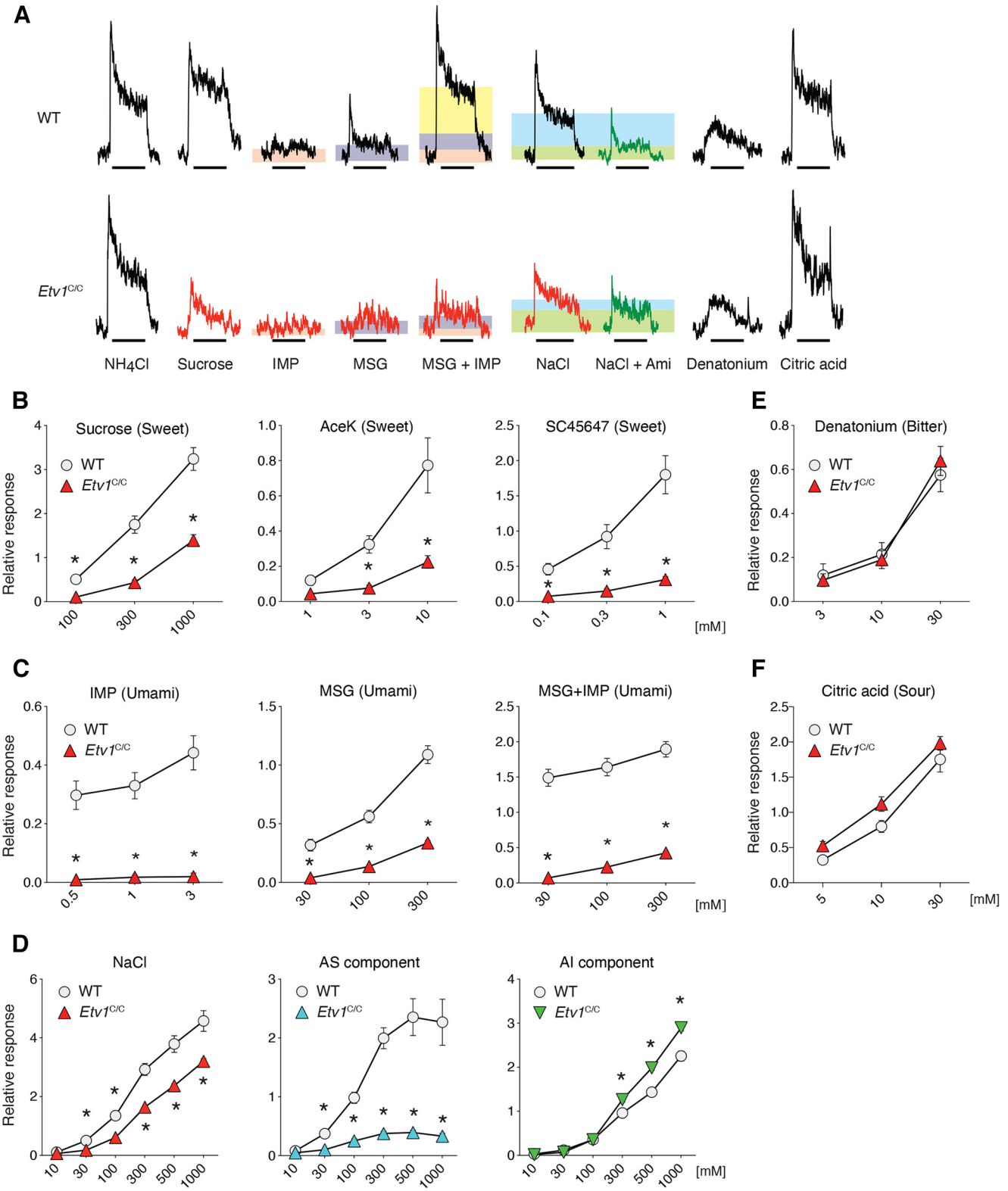

Figure 9. Etv1 deficiency in taste cells impairs neural responses to sweet, umami, and sodium tastes. ***A***, Representative charts of chorda tympani nerve responses of wild-type (WT; top) and *Etv1*$^{C/C}$ (bottom) mice to taste solutions: 100 mM NH_4Cl, 300 mM sucrose, 0.5 mM inositol monophosphate (IMP), 100 mM monosodium glutamate (MSG), 100 mM MSG with 0.5 mM IMP, 100 mM sodium chloride (NaCl), 100 mM NaCl with 100 μM amiloride (Ami), 30 mM denatonium, and 10 mM citric acid. Responses of 0.5 mM IMP (orange) and 100 mM MSG (purple) are depicted as shaded rectangles to clarify the synergy (yellow) in the response of 100 mM MSG with 0.5 mM IMP. Responses to NaCl are depicted as shaded rectangles for amiloride-sensitive (blue) and amiloride-insensitive

continued

(green) components. The bars under the traces show the duration (30 s) of the taste stimulus. ***B***, Whole chorda tympani nerve responses of WT and *Etv1*$^{C/C}$ mice to sweet taste solutions. Left, Sucrose. Middle, Acesulfame K (AceK). Right, SC45647. ***C***, Whole chorda tympani nerve responses of wild-type and *Etv1*$^{C/C}$ mice to umami taste solutions. Left, IMP. Middle, MSG. Right, MSG with 0.5 mM IMP. ***D***, Whole chorda tympani nerve responses of WT and *Etv1*$^{C/C}$ mice to NaCl solutions. Amiloride-sensitive salt responses (AS component; middle) are measured by subtracting the amiloride-insensitive response (AI component; right) from the whole salt response (left). ***E***, ***F***, Whole chorda tympani nerve responses of WT (circles) and *Etv1*$^{C/C}$ (triangles) mice to bitter (***E***) and sour (***F***) taste solutions that are received by receptors other than T1Rs ($n = 8$ for each genotype). Significance was assessed by repeated-measures two-way ANOVA and the Sidak's multiple comparison test. *Significantly different ($p < 0.05$) responses between genotypes. Data are expressed as the mean ± SEM; where error bars are not visible, they are smaller than the symbol depicting the mean. See Table 3 for statistical values.

regional discrepancy may be explained by the different degrees of compensation by distinct, yet-to-be-identified transcription regulators that cooperate with Etv1 in sweet, umami, and sodium taste cells, as discussed above. Because these taste cells differ in their spatial distributions (Hoon et al., 1999; Chandrashekar et al., 2010; Ohmoto et al., 2020a), regional differences in impacts of Etv1 deficiency are perhaps unsurprising.

Many genes that encode transcription factors involved in the regulation of gene expression are expressed in taste buds (Hevezi et al., 2009; Lee et al., 2017; Sukumaran et al., 2017). Some of them may play crucial roles in specifying respective taste cells and maintaining their specific identities. Like Sox2 in stem cells and Skn-1a in precursor cells, several factors would act as selectors at several crossroads in the differentiation process of taste bud cells. It would be very interesting to identify which transcription factor genes are expressed in which taste cells by single-cell RNAseq and to analyze which genes' 5'-upstream regions are accessible

Table 3: Summary of statistical analyses of chorda tympani responses of wild-type (WT) and *Etv1*$^{C/C}$ mice to taste compounds

Quality	Compound (component)	Genotype (WT vs *Etv1*$^{C/C}$)		Concentration		Interaction		Concentration differing significantly with p value*
Sweet	Sucrose	$F_{(1,14)} = 43.3$	$p < 0.0001$	$F_{(1.274,17.83)} = 249.2$	$p < 0.0001$	$F_{(2,28)} = 32.5$	$p < 0.0001$	100 mM ($p = 0.0023$) 300 mM ($p = 0.0005$) 1000 mM ($p = 0.0002$)
	Acesulfame K	$F_{(1,14)} = 15.9$	$p = 0.0014$	$F_{(1.072,15.01)} = 27.26$	$p < 0.0001$	$F_{(2,28)} = 8.5$	$p = 0.0013$	3 mM ($p = 0.0036$) 10 mM ($p = 0.028$)
	SC45647	$F_{(1,14)} = 26.0$	$p = 0.0002$	$F_{(1.269,17.76)} = 58.94$	$p < 0.0001$	$F_{(2,44)} = 52.3$	$p < 0.0001$	0.1 mM ($p = 0.0064$) 0.3 mM ($p = 0.0075$) 1 mM ($p = 0.0025$)
Umami	Inosine monophosphate (IMP)	$F_{(1,14)} = 48.9$	$p < 0.0001$	$F_{(1.759,24.63)} = 15.34$	$p < 0.0001$	$F_{(2,28)} = 12.1$	$p = 0.0002$	0.5 mM ($p = 0.0016$) 1 mM ($p = 0.0005$) 3 mM ($p = 0.0004$)
	Monosodium glutamate (MSG)	$F_{(1,14)} = 68.5$	$p < 0.0001$	$F_{(1.669,23.37)} = 408.9$	$p < 0.0001$	$F_{(2,28)} = 80.6$	$p < 0.0001$	30 mM ($p = 0.0020$) 100 mM ($p = 0.0002$) 300 mM ($p < 0.0001$)
	MSG+IMP[a]	$F_{(1,14)} = 172.0$	$p < 0.0001$	$F_{(1.340,18.76)} = 43.54$	$p < 0.0001$	$F_{(2,28)} = 0.28$	$p = 0.76$	30 mM ($p < 0.0001$) 100 mM ($p < 0.0001$) 300 mM ($p < 0.0001$)
Salty[b]	NaCl	$F_{(1,14)} = 33.3$	$p < 0.0001$	$F_{(1.881,26.33)} = 347.0$	$p < 0.0001$	$F_{(5,70)} = 12.4$	$p < 0.0001$	30 mM ($p = 0.0013$) 100 mM ($p = 0.0007$) 300 mM ($p = 0.0022$) 500 mM ($p = 0.0081$) 1000 mM ($p = 0.033$)
	(AS salt)	$F_{(1,14)} = 53.6$	$p < 0.0001$	$F_{(1.704,23.85)} = 38.07$	$p < 0.0001$	$F_{(5,70)} = 21.7$	$p < 0.0001$	30 mM ($p = 0.0059$) 100 mM ($p = 0.0003$) 300 mM ($p = 0.0002$) 500 mM ($p = 0.0024$) 1000 mM ($p = 0.0095$)
	(AI salt)	$F_{(1,14)} = 20.3$	$p = 0.0005$	$F_{(1.637,22.92)} = 1060$	$p < 0.0001$	$F_{(5,70)} = 23.9$	$p < 0.0001$	300 mM ($p = 0.0029$) 500 mM ($p = 0.0006$) 1000 mM ($p = 0.0026$)
Bitter	Denatonium	$F_{(1,14)} = 0.0072$	$p = 0.93$	$F_{(1.224,17.13)} = 119.8$	$p < 0.0001$	$F_{(2,28)} = 1.1$	$p = 0.35$	
Sour	Citric acid	$F_{(1,14)} = 3.9$	$p = 0.068$	$F_{(1.368,19.15)} = 230.8$	$p < 0.0001$	$F_{(2,28)} = 0.4$	$p = 0.67$	

*$p < 0.05$ according to *post hoc* Sidak's multiple comparison test.
[a] MSG solutions with 0.5 mM IMP.
[b] Responses to NaCl were recorded in the absence and presence of amiloride so that amiloride-sensitive (AS) salt responses were calculated by subtracting amiloride-insensitive (AI) responses from whole NaCl responses.

for transcription machinery in individual taste cells by single-cell ATAC-seq.

Tissue-specific or cell-specific isoforms of Etv1

The *Etv1* mutant strain used in this study, $Etv1^{C/C}$, is designed to encode a tamoxifen-inducible Cre recombinase CreER instead of Etv1, analogous to another *Etv1* mutant strain, $Etv1^{nlslacZ/nlslacZ}$, which is designed to encode a nuclear-localized β-galactosidase (Extended Data Fig. 2-1*A*; Arber et al., 2000; Taniguchi et al., 2011). Therefore, these two strains were expected to exhibit similar phenotypes: impaired locomotion because of deficits in proprioceptive neuronal circuits, and a short life span (up to several weeks), as observed in $Etv1^{nlslacZ/nlslacZ}$ mice, in which Etv1-like immunoreactivity was remarkably reduced in DRG neurons (Arber et al., 2000). However, $Etv1^{C/C}$ mice exhibit no overt abnormality in locomotion, and this strain can be maintained as homozygous. More notable, Etv1-like immunoreactivity in DRG in $Etv1^{C/C}$ mice is observed in the proprioceptive sensory neurons, comparable to wild-type mice (Fig. 2). Also, qualitative and quantitative PCR analyses demonstrated no significant change of *Etv1*-derived transcript in DRG in $Etv1^{C/C}$ mice, consistent with qualitative observations by *in situ* hybridization analyses. However, no cDNA fragment was amplified from N-terminal coding exons, probably because transcription from the first exon of *Etv1* is stopped by the insertion of CreERT2 in the second exon (Extended Data Fig. 2-1*C*). The fact that *Etv1*-v2 detected as a major transcript in DRG by 5'-RACE starts its transcription from the sequence in the fourth intron of *Etv1* (Extended Data Fig. 2-1*B*,*C*) can account for little, if any, impact on its expression by CreERT2 insertion. The discrepancy of *Etv1*-v2 expression level between $Etv1^{nlslacZ/nlslacZ}$ and $Etv1^{C/C}$ mice may be attributed to the remaining *pgk-Neo* sequence in the *Etv1* locus of $Etv1^{nlslacZ/nlslacZ}$ mice (Extended Data Fig. 2-1*A*), as reported in other alleles (Fernex et al., 1997; Nagy et al., 1998; Kist et al., 2005; Joo et al., 2007; Andersen et al., 2014).

Intriguingly, *Etv1*-derived transcripts are also expressed in putative gustatory neurons in GG in wild-type and $Etv1^{C/C}$ mice, but unlike in proprioceptive neurons in DRG and in taste cells, in GG in $Etv1^{C/C}$ mice the expression of *Etv1*-derived transcripts is significantly decreased but not lost. Species and amounts of Etv1 isoforms seem to vary among cells and/or tissues. Identifying isoforms and examining the phenotypes in $Etv1^{+}$ cells in $Etv1^{C/C}$ mice may provide insights into structure-function relationships of Etv1. For example, because Etv1 is absent in DRG in $Etv1^{C/C}$ mice, which do not display impaired locomotion or proprioception, such phenotypes observed in $Etv1^{nlslacZ/nlslacZ}$ and $Etv1^{ETS/ETS}$ mice can be attributable to the loss of Etv1 isoform b encoded by *Etv1*-v2 in proprioceptive neurons but not to the loss of Etv1, although they may be functionally redundant. It is suggested that Etv1 is involved in different processes in multiple malignant tissues, such as carcinogenesis of prostate cancer, cell survival of gastrointestinal stromal tumor, and metastasis of pancreatic cancer (Tomlins et al., 2005; Chi et al., 2010; Heeg et al., 2016). It may be not Etv1 but an isoform that is involved in those pathologic conditions. $Etv1^{C/C}$ mice, together with $Etv1^{nlslacZ/nlslacZ}$ and $Etv1^{EST/EST}$ mice, will be very valuable models to understand how Etv1 and its isoforms are involved in those processes in cancer studies, in addition to studying their roles in normal adult tissues.

References

Abe H, Okazawa M, Nakanishi S (2011) The Etv1/Er81 transcription factor orchestrates activity-dependent gene regulation in the terminal maturation program of cerebellar granule cells. Proc Natl Acad Sci U S A 108:12497–12502.

Andersen J, Urbán N, Achimastou A, Ito A, Simic M, Ullom K, Martynoga B, Lebel M, Göritz C, Frisén J, Nakafuku M, Guillemot F (2014) A transcriptional mechanism integrating inputs from extracellular signals to activate hippocampal stem cells. Neuron 83: 1085–1097.

Arber S, Ladle DR, Lin JH, Frank E, Jessell TM (2000) ETS gene Er81 controls the formation of functional connections between group Ia sensory afferents and motor neurons. Cell 101:485–498.

Beidler LM, Smallman RL (1965) Renewal of cells within taste buds. J Cell Biol 27:263–272.

Chandrashekar J, Kuhn C, Oka Y, Yarmolinsky DA, Hummler E, Ryba NJP, Zuker CS (2010) The cells and peripheral representation of sodium taste in mice. Nature 464:297–301.

Chi P, Chen Y, Zhang L, Guo X, Wongvipat J, Shamu T, Fletcher JA, Dewell S, Maki RG, Zheng D, Antonescu CR, Allis CD, Sawyers CL (2010) ETV1 is a lineage survival factor that cooperates with KIT in gastrointestinal stromal tumours. Nature 467:849–853.

Dvoryanchikov G, Hernandez D, Roebber JK, Hill DL, Roper SD, Chaudhari N (2017) Transcriptomes and neurotransmitter profiles of classes of gustatory and somatosensory neurons in the geniculate ganglion. Nat Commun 8:760.

Farbman AI (1980) Renewal of taste bud cells in rat circumvallate papillae. Cell Tissue Kinet 13:349–357.

Fernex C, Dubreuil P, Mannoni P, Bagnis C (1997) Cre/loxP-mediated excision of a neomycin resistance expression unit from an integrated retroviral vector increases long terminal repeat-driven transcription in human hematopoietic cells. J Virol 71:7533–7540.

Finger TE, Danilova V, Barrows J, Bartel DL, Vigers AJ, Stone L, Hellekant G, Kinnamon SC (2005) ATP signaling is crucial for communication from taste buds to gustatory nerves. Science 310:1495–1499.

Fleming MS, Li JJ, Ramos D, Li T, Talmage DA, Abe SI, Arber S, Luo W (2016) A RET-ER81-NRG1 signaling pathway drives the development of Pacinian corpuscles. J Neurosci 36:10337–10355.

Guagliardo NA, Hill DL (2007) Fungiform taste bud degeneration in C57BL/6J mice following chorda-lingual nerve transection. J Comp Neurol 504:206–216.

Guth L (1957) The effects of glossopharyngeal nerve transection on the circumvallate papilla of the rat. Anat Rec 128:715–731.

Heeg S, Das KK, Reichert M, Bakir B, Takano S, Caspers J, Aiello NM, Wu K, Neesse A, Maitra A, Iacobuzio-Donahue CA, Hicks P, Rustgi AK (2016) ETS-transcription factor ETV1 regulates stromal expansion and metastasis in pancreatic cancer. Gastroenterology 151:540–553.e14.

Hevezi P, Moyer BD, Lu M, Gao N, White E, Echeverri F, Kalabat D, Soto H, Laita B, Li C, Yeh SA, Zoller M, Zlotnik A (2009) Genome-wide analysis of gene expression in primate taste buds reveals links to diverse processes. PLoS One 4:e6395.

Hoon MA, Adler E, Lindemeier J, Battey JF, Ryba NJP, Zuker CS (1999) Putative mammalian taste receptors: a class of taste-specific GPCRs with distinct topographic selectivity. Cell 96:541–551.

Huang AL, Chen X, Hoon MA, Chandrashekar J, Guo W, Tränkner D, Ryba NJP, Zuker CS (2006) The cells and logic for mammalian sour taste detection. Nature 442:934–938.

John SJS, Garcea M, Spector AC (2003) The time course of taste bud regeneration after glossopharyngeal or greater superficial petrosal nerve transection in rats. Chem Senses 28:33–43.
Joo JH, Lee YJ, Munguba GC, Park S, Taxter TJ, Elsagga MY, Jackson MR, Oh SP, Sugrue SP (2007) Role of Pinin in neural crest, dorsal dermis, and axial skeleton development and its involvement in the regulation of Tcf/Lef activity in mice. Dev Dyn 236:2147–2158.
Kennedy JG (1972) The effects of transection of the glossopharyngeal nerve on the taste buds of the circumvallate papilla of the rat. Arch Oral Biol 17:1197–1207.
Kist R, Watson M, Wang X, Cairns P, Miles C, Reid DJ, Peters H (2005) Reduction of Pax9 gene dosage in an allelic series of mouse mutants causes hypodontia and oligodontia. Hum Mol Genet 14:3605–3617.
Lee H, Macpherson LJ, Parada CA, Zuker CS, Ryba NJP (2017) Rewiring the taste system. Nature 548:330–333.
Livak KJ, Schmittgen TD (2001) Analysis of relative gene expression data using real-time quantitative PCR and the $2^{\Delta\Delta-CT}$ method. Methods 25:402–408.
Madisen L, Zwingman TA, Sunkin SM, Oh SW, Zariwala HA, Gu H, Ng LL, Palmiter RD, Hawrylycz MJ, Jones AR, Lein ES, Zeng H (2010) A robust and high-throughput Cre reporting and characterization system for the whole mouse brain. Nat Neurosci 13:133–140.
Matsumoto I, Ohmoto M, Narukawa M, Yoshihara Y, Abe K (2011) Skn-1a (Pou2f3) specifies taste receptor cell lineage. Nat Neurosci 14:685–687.
Matsumoto I, Ohmoto M, Abe K (2013) Functional diversification of taste cells in vertebrates. Semin Cell Dev Biol 24:210–214.
Mueller KL, Hoon MA, Erlenbach I, Chandrashekar J, Zuker CS, Ryba NJP (2005) The receptors and coding logic for bitter taste. Nature 434:225–229.
Nagy A, Moens C, Ivanyi E, Pawling J, Gertsenstein M, Hadjantonakis A-K, Pirity M, Rossant J (1998) Dissecting the role of N-myc in development using a single targeting vector to generate a series of alleles. Curr Biol 8:661–664.
Nelson G, Hoon MA, Chandrashekar J, Zhang Y, Ryba NJP, Zuker CS (2001) Mammalian sweet taste receptors. Cell 106:381–390.
Nelson G, Chandrashekar J, Hoon MA, Feng L, Zhao G, Ryba NJP, Zuker CS (2002) An amino-acid taste receptor. Nature 416:199–202.
Nomura K, Nakanishi M, Ishidate F, Iwata K, Taruno A (2020) All-electrical Ca^{2+}-independent signal transduction mediates attractive sodium taste in taste buds. Neuron 106:816–829.e6.
Ohmoto M, Matsumoto I, Yasuoka A, Yoshihara Y, Abe K (2008) Genetic tracing of the gustatory and trigeminal neural pathways originating from T1R3-expressing taste receptor cells and solitary chemoreceptor cells. Mol Cell Neurosci 38:505–517.
Ohmoto M, Ren W, Nishiguchi Y, Hirota J, Jiang P, Matsumoto I (2017) Genetic lineage tracing in taste tissues using Sox2-CreERT2 strain. Chem Senses 42:547–552.
Ohmoto M, Jyotaki M, Foskett JK, Matsumoto I (2020a) Sodium taste cells require Skn-1a for generation and share molecular features with sweet, umami, and bitter taste cells. eNeuro 7: ENEURO.0385-20.2020.
Ohmoto M, Lei W, Yamashita J, Hirota J, Jiang P, Matsumoto I (2020b) SOX2 regulates homeostasis of taste bud cells and lingual epithelial cells in posterior tongue. PLoS One 15:e0240848.
Ohmoto M, Kitamoto S, Hirota J (2021) Expression of Eya1 in mouse taste buds. Cell Tissue Res 383:979–986.
Okazawa M, Abe H, Nakanishi S (2016) The Etv1 transcription factor activity-dependently downregulates a set of genes controlling cell growth and differentiation in maturing cerebellar granule cells. Biochem Biophys Res Commun 473:1071–1077.
Patel TD, Kramer I, Kucera J, Niederkofler V, Jessell TM, Arber S, Snider WD (2003) Peripheral NT3 signaling is required for ETS protein expression and central patterning of proprioceptive sensory afferents. Neuron 38:403–416.
Ren W, Lewandowski BC, Watson J, Aihara E, Iwatsuki K, Bachmanov AA, Margolskee RF, Jiang P (2014) Single Lgr5- or Lgr6-expressing taste stem/progenitor cells generate taste bud cells ex vivo. Proc Natl Acad Sci U S A 111:16401–16406.
Stone LM, Finger TE, Tam PPL, Tan S-S (1995) Taste receptor cells arise from local epithelium, not neurogenic ectoderm. Proc Natl Acad Sci U S A 92:1916–1920.
Sukumaran S, Lewandowski B, Qin Y, Kotha R, Bachmanov AA, Margolskee RF (2017) Whole transcriptome profiling of taste bud cells. Sci Rep 7:7595.
Takeda N, Jain R, Li D, Li L, Lu MM, Epstein JA (2013) Lgr5 identifies progenitor cells capable of taste bud regeneration after injury. PLoS One 8:e66314.
Taniguchi H, He M, Wu P, Kim S, Paik R, Sugino K, Kvitsiani D, Fu Y, Lu J, Lin Y, Miyoshi G, Shima Y, Fishell G, Nelson SB, Huang ZJ (2011) A resource of Cre driver lines for genetic targeting of GABAergic neurons in cerebral cortex. Neuron 71:995–1013.
Taruno A, Vingtdeux V, Ohmoto M, Ma Z, Dvoryanchikov G, Li A, Adrien L, Zhao H, Leung S, Abernethy M, Koppel J, Davies P, Civan MM, Chaudhari N, Matsumoto I, Hellekant G, Tordoff MG, Marambaud P, Foskett JK (2013) CALHM1 ion channel mediates purinergic neurotransmission of sweet, bitter and umami tastes. Nature 495:223–226.
Tomlins SA, Rhodes DR, Perner S, Dhanasekaran SM, Mehra R, Sun X-W, Varambally S, Cao X, Tchinda J, Kuefer R, Lee C, Montie JE, Shah RB, Pienta KJ, Rubin MA, Chinnaiyan AM (2005) Recurrent fusion of TMPRSS2 and ETS transcription factor genes in prostate cancer. Science 310:644–648.
Yarmolinsky DA, Zuker CS, Ryba NJP (2009) Common sense about taste: from mammals to insects. Cell 139:234–244.
Zhao GQ, Zhang Y, Hoon MA, Chandrashekar J, Erlenbach I, Ryba NJP, Zuker CS (2003) The receptors for mammalian sweet and umami taste. Cell 115:255–266.